REVIEW ARTICLE

Technological solutions for NO_x, SO_x, and VOC abatement: recent breakthroughs and future directions

Aathira Bhaskaran[1] · Deepika Sharma[2] · Sounak Roy[1,3] · Satyapaul A. Singh[3,4]

Abstract

NO_x, SO_x, and carbonaceous volatile organic compounds (VOCs) are extremely harmful to the environment, and their concentrations must be within the limits prescribed by the region-specific pollution control boards. Thus, NO_x, SO_x, and VOC abatement is essential to safeguard the environment. Considering the importance of NO_x, SO_x, and VOC abatement, the discussion on selective catalytic reduction, oxidation, redox methods, and adsorption using noble metal and non-noble metal-based catalytic approaches were elaborated. This article covers different thermal treatment techniques, category of materials as catalysts, and its structure–property insights along with the advanced oxidation processes and adsorption. The defect engineered catalysts with lattice oxygen vacancies, bi- and tri-metallic noble metal catalysts and non-noble metal catalysts, modified metal organic frameworks, mixed-metal oxide supports, and their mechanisms have been thoroughly reviewed. The main hurdles and potential achievements in developing novel simultaneous NO_x, SO_x, and VOC removal technologies are critically discussed to envisage the future directions. This review highlights the removal of NO_x, SO_x, and VOC through material selection, properties, and mechanisms to further improve the existing abatement methods in an efficient way.

Keywords NO_x reduction · SO_x reduction · VOC abatement · SCR · SCO · LDO (layered double oxide) · Photocatalysis

Responsible Editor: George Z. Kyzas

Aathira Bhaskaran and Deepika Sharma contributed equally to this work.

✉ Satyapaul A. Singh
satyapaul@hyderabad.bits-pilani.ac.in

1 Department of Chemistry, Birla Institute of Technology and Science Pilani, Hyderabad Campus, Hyderabad 500078, India

2 Department of Chemical Engineering, Birla Institute of Technology and Science Pilani, Pilani Campus, Pilani 333031, India

3 Materials Center for Sustainable Energy & Environment, Birla Institute of Technology and Science Pilani Hyderabad Campus, Hyderabad 500078, India

4 Department of Chemical Engineering, Birla Institute of Technology and Science Pilani, Hyderabad Campus, Hyderabad 500078, India

Introduction

Industrial revolution and growing global energy needs have been the prominent cause of air pollution. Uncontrolled release of pollutants and emissions contribute to global warming, climate change, acid rain, and other environmental changes (Munsif et al. 2021). These emissions include SO_x, NO_x, volatile organic compound (VOC), and CO emissions which are primary pollutants and are directly produced from industrial processes (Roberts 2021). VOCs react with NO_x (mainly nitrogen dioxide) to form fine particles or secondary pollutants and accumulation of these secondary pollutants (ozone, fine particulates) causes smog. Apart from affecting the environment, adverse health effects are possible with emissions. According to a report by the economic consequences of outdoor air pollution, the worrying situation of air pollution is increasing premature deaths. The Organization for Economic Co-operation and Development's (OECD) ENV-Linkages model, a computable general equilibrium (CGE) model, suggests the possibility of increase in deaths from 3 to 9 million in a span of 2010 to 2060. The number of premature deaths is unequally distributed across the world. The highest number of deaths takes place in non-OECD

economies and particularly in China and India. Other major impacts of air pollution are as follows: reduced labor productivity, increased health expenditures and crop yields. Globally these impacts continue to increase significantly relative to gross domestic product (GDP). In contrast, agricultural impacts are relatively stable over time in percentage of GDP, i.e., in absolute terms these impacts grow more or less at the same speed as GDP. Taken together, the total annual market costs of outdoor air pollution are projected to rise from 0.3% in 2015 to 1.0% by 2060 (Highlights 1978).

Major pollutant like carbon monoxide emissions can directly cause poisoning when intake reaches high ppm levels and other emissions are responsible for respiratory problems like asthma, central nervous systems diseases, chronic pulmonary disease, and cardiovascular diseases occur in individuals with long-term exposure to air pollution. Repeated exposure to them can also lead to skin-related problems like melisma and photodamage. Prolonged exposure to NO_x and SO_x can cause breathing issue, bronchospasm, and pulmonary edema. Exposure to VOCs can cause headache, nausea, and along with respiratory issues. The longer exposure to the compound can affect liver and kidney and can even cause cancer (Puri et al. 2017; Manisalidis et al. 2020; Shi et al. 2021a, d). Damage up to this extent mainly occurs in urban and industrial areas due to industrial emissions and vehicular emissions (Ma et al. 2021b). To decrease such adverse effects, several countries have set up emission standards for industries and automobiles so that these emissions are limited. As of 2020, 124 countries (about two thirds) were found to have national ambient air quality standards which is 17% more than reported in 2016. However, only 9% of these adhere to the limits established by the World Health Organization (WHO) guidelines.

US Environmental Protection Agency implemented National Ambient Air Quality Standards where there are limits for each pollutant. Similarly, South Korea follows Clean Air Conservation Act and Japan follows Environmental Quality Standards for air pollution limits. Also, several countries have set up emission standards for industries and automobiles so that these emissions are limited. There is a standard for automobile emission where the current standard follows Euro 6 by most of the countries including South Korea, European Union, Thailand, Indonesia, etc. The Central Pollution Control Board (CPCB) of India has set emission standards for 31 categories of industries for control of air pollution. Different standards and concentration limits of the pollutants are explained in Table 1. Therefore, the need to render these pollutants harmless before releasing them into the environment is extremely important, for which several treatment technologies have to be implemented.

Types of emissions

NO_x

Nitric acid and nitrogen dioxide (NO and NO_2) are major contributors to air pollution and take a part in global warming and greenhouse effect. Industrial sources include power

Table 1 Pollutant concentration and standards in different countries

Country	Regulating body	Current standards	Emission limits for light vehicles (compression engine-diesel) (g km^{-1})				
			CO	HC	HC+NO_x	NO_x	PM
USA	US Environmental Protection Agency (EPA)	Tier 3 50,000 miles/5 years	3.4	0.41	–	1.0	0.08
South Korea	Ministry of Environment	Euro 6	0.74	–	0.215	0.125	0.0045
Japan	Ministry of the Environment (MOE)	New Post Long-Term Standards	0.63	0.02	–	0.15	0.007
China	Ministry of Ecology and Environment	China 5 (parallel to Euro 5), GB 18352.5–2013	0.7	0.1	–	0.06	0.0045
EU	European Union	Euro 6 for all vehicle sales and registrations	0.50	–	0.17	0.08	0.005
India	Central Pollution Control Board (CPCB)	Bharat III nationwide, Bharat IV in select states and cities (parallel to Euro standards)	0.74	0.1	0.215	0.125	0.0045
Russia	Federal Agency for Technical Regulating and Metrology	Euro V	1	0.1	–	0.06	0.0045
Vietnam	Ministry of Transport	Euro 5 as adopted under No. 49/2011/QD-TTg	0.74	–	0.35	0.28	0.0045
Canada	Environment and Climate Change Canada	Tier 2 in 2003 On-Road Vehicle and Engine Emission Regulations (g/mile)	7.3	0.032	–	0.9	0.12
Australia	Department of Infrastructure and Regional Development	ADR79/03, equivalent to Euro 5	0.74	–	0.215	0.125	0.0045

plants, industrial boilers, cement kilns, turbines, and other major sources are automobiles. Another oxide of nitrogen, N_2O has 300 times higher greenhouse impact on a per molecular basis than carbon dioxide (Boningari and Smirniotis 2016; Skowron et al. 2021). They have adverse effects on human health too and therefore strict regulations and standards have been set up to limit NO_x emissions which might have to be tightened further in future (Liu et al. 2018). Several methods have been found for NO_x abatement but many of them are complex, produce undesirable products, and are not cost-effective (Roy et al. 2009; Martinez-Oviedo et al. 2021). Selective catalytic reduction (SCR) in presence of ammonia is one of the most effective ways for control of industrial NO_x emissions (Tian et al. 2021a).

SO_x

SO_x emissions are majorly caused by combustion of fossil fuels at industries and power plants. SO_x have acidifying effect and can harm both land and water by means of acid rain thereby reducing the growth of plants. Also, it can affect the respiratory tract and can cause lung infection (Jiang et al. 2011; Liu and Guo 2021). For SO_x abatement, several pre-combustion and post-combustion techniques can be used like pressurized fluidized bed combustion which provides to about 98% SO_2 reduction and sorbents can be used for removal of SO_x (Rahmaninejad et al. 2012).

Carbon compound emissions

VOCs are all organic chemicals that include compounds of carbon. They also play a role in formation of secondary organic aerosols via photo-oxidation along with nitrogen oxides and sunlight which are found in airborne particulate matter and are the key precursors in formation of ground level ozone (Atkinson and Arey 2003). As far as human health is concerned, BTEX (group of VOCs of benzene, toluene, ethylbenzene, and xylenes) have carcinogenic effects and can lead to toxicity on inhalation even at low concentrations. Other health effects include headache, neurological diseases, eye irritation, etc. (Ueno et al. 2001; Kampa and Castanas 2008, 2018). Owing to stringent regulations, VOC abatement treatments have gained importance in the past few years and catalytic oxidation is regarded as one of the most efficient and promising approaches for VOC removal (Wu et al. 2016; Méausoone et al. 2019; Liu et al. 2021). Other major pollutant is carbon monoxide (CO) and carbon dioxide (CO_2) which is present as a pollutant in troposphere and plays a significant role in global carbon cycle and greenhouse effect (Streets et al. 2006; Jiang et al. 2015). Catalytic oxidation and water–gas shift reactions are promising methods for CO abatement (Gokhale et al. 2008; Zhu and Wachs 2015; Chen and Chen 2020), where normally in water–gas

shift reaction, CO reacts with water to form CO_2 and H_2. CO_2 hydrogenation and reforming reactions are helpful to address CO_2 abatement, where in reforming, CO_2 reacts with CH_4 to give syngas (Kathiraser et al. 2015; Cai and Hu 2019; Yang et al. 2019; Neha and Vir Singh 2020). However, in this review, our discussion is limited to NO_x, SO_x, and VOC abatement.

Treatment technologies

The research and adaptation of promising, cost-effective methods for industrial emission control have taken a faster pace in the past few years. A lot of technologies like photocatalysis (Roy et al. 2007b, a), catalytic ozonation (which is more cost effective in comparison to single ozonation), plasma catalysis, selective catalytic reduction/oxidation, storage and reduction (Roy and Baiker 2009; Roy et al. 2010, 2012), and adsorption are found to be effective methodologies. For automobile and vehicular emissions, control catalytic converters prove to be a promising method (Casagrande et al. 2020; Guo et al. 2020; Naveenkumar et al. 2020; Li et al. 2021c; Shang et al. 2021; Wang et al. 2021b; Tan et al. 2022).

Catalytic oxidation/reduction

Techniques such as catalytic oxidation, selective catalytic reduction, and selective catalytic oxidation occurs in presence of catalysts that decrease the activation energy, thereby increases the rate of reactions. Packed and fluidized bed catalytic reactors are found to be economically feasible, produces low concentrations of secondary pollutants at large scale, and can occur at low temperatures than other treatment methods (Zhao et al. 2020b; Guo et al. 2021b; Li et al. 2021b). As most of the catalysts require high temperatures for the emission removal, the obvious energy needs become greater and which significantly increases the operating cost of the process. Hence, research on the development of efficient catalysts is essential to bring down the operating costs. The catalytic efficiency can be increased in several ways such as tuning the catalyst preparative method, doping the active metal over other oxides/metals or by changing the support of the catalyst and modifying the catalyst morphology (Roy et al. 2007d, c, 2008c; Roy and Hegde 2008; Jurado et al. 2021; Zhang et al. 2021c). Recently, a lot of focus has been laid upon research of low temperature catalysts because of high return and low operational cost. Figure 1 shows the number of published research papers on low-temperature reactions from 2000 to 2021 as obtained from Scopus data. It indicates the growing scientific interest on pollution control through catalytic routes.
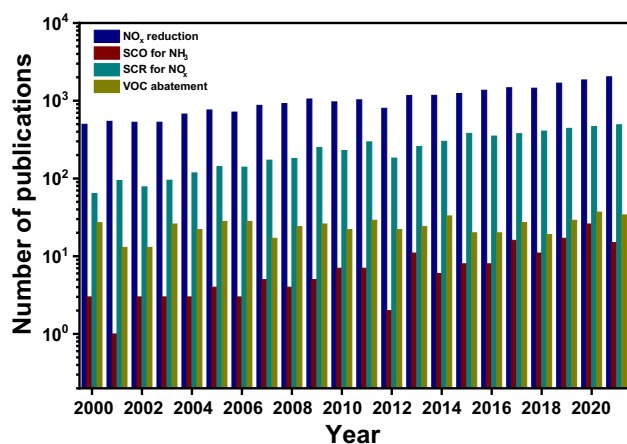
Fig. 1 Number of published research papers on low-temperature reactions

Adsorption

Adsorption is widely recognized as a highly effective and non-destructive method for the removal of volatile organic compounds (VOCs) and nitrogen oxides (NO_x). It offers several advantages, including the ability to recover and reuse the adsorbed VOCs, making it an environmentally friendly approach. This has led to increased attention on commercially available adsorbents such as activated carbon, silica gel, biochar, and zeolites, which have proven to be highly efficient and cost-effective options for adsorption processes. Activated carbon is one of the most commonly used adsorbents due to its large surface area and high adsorption capacity. It exhibits excellent performance in removing a wide range of VOCs and NO_x from various sources. Silica gel, another popular adsorbent, possesses a high affinity for polar molecules and is particularly effective in adsorbing moisture and certain types of VOCs. Biochar, derived from biomass pyrolysis, has emerged as a promising adsorbent in recent years. Its porous structure and surface chemistry make it suitable for VOC and NO_x adsorption. Zeolites, with their well-defined pore structure and high thermal stability, are also extensively utilized for adsorption applications. They exhibit selective adsorption properties for specific VOCs and have shown remarkable performance in pollutant removal. Research studies conducted by Wu et al. (2019; Wu et al. 2021; Zhang et al. 2021a) have further highlighted the effectiveness of these adsorbents in VOC and NO_x removal. Their findings demonstrate the successful application of these materials in various industries, emphasizing the potential of adsorption as a reliable and efficient technique.

Redox methods

Several advanced oxidation processes (AOPs) with good prospects for developing air cleaning technologies are UV/ozonation, H_2O_2/ozonation, or photocatalysis. The advantage of photocatalysis implementation in indoor air treatment is given by the absence of additional oxidizers (such as H_2O_2). The photocatalysis can occur at low temperatures and catalyst is used for longer hours (Sekiguchi et al. 2010; Challagulla et al. 2019).

The present comprehensive review aims to provide a consolidated overview of recent advancements in the field of NO_x, SO_x, and VOC abatement through catalysis. Though there are several review articles on NO_x reduction and VOC abatements (He et al. 2019; Chen et al. 2021a; Zhao et al. 2022; Li et al. 2023), here we present a review which encompasses a wide range of topics, including NO_x, SO_x reduction, and VOC abatement by advanced catalysis techniques and adsorption. The development and optimization of catalytic materials play a vital role in achieving efficient and sustainable reduction of harmful emissions, contributing to improved air quality and a healthier environment. The performance characteristics of noble metal and non-noble metal catalysts are dealt in this study in the controlling mechanism point of view. The effect of mono-, bi-, and tri-metallic dopants on the reaction mechanism is also investigated. Further, redox and adsorption methods are also investigated for the removal of toxic gases. This will enable the researchers to choose a suitable material to abate the harmful gases in terms of energy efficiency, abundancy, and economics for catalytic/non-catalytic processes. By providing an amalgamated overview of the recent progress made in the field, this report aims to enhance understanding and knowledge regarding the significant role played by catalysis in the abatement of NO_x, SO_x, and VOCs, paving the way for further research and technological advancements in the field. A detailed schematic on the abatement technologies for NO_x/SO_x, VOC is shown in Fig. 2.

SCR for NO_x removal

SCR is seen as an efficient method for NO_x reduction to N_2. Commercially used catalysts operate at 300–400 °C. But at higher operating temperature, sulfur contamination in the feed can cause sintering of the catalyst and affect its stability. Thus, sulfur-tolerant and low-temperature SCR is a welcoming strategy with efficient catalysts (Pappas et al. 2016; Yan et al. 2021). The demand for efficient NO_x removal has led to the development of several classes of SCR catalysts. SCR mainly involves three reactions named as standard SCR, fast SCR, and NO_2-SCR (Zhou et al. 2020). SCR can be categorized into noble metal based (Pt, Pd, Au, Ag) and non-noble

Fig. 2 Schematic diagram explaining the NO_x, SO_x, VOC emission effects and solution by abatement technologies
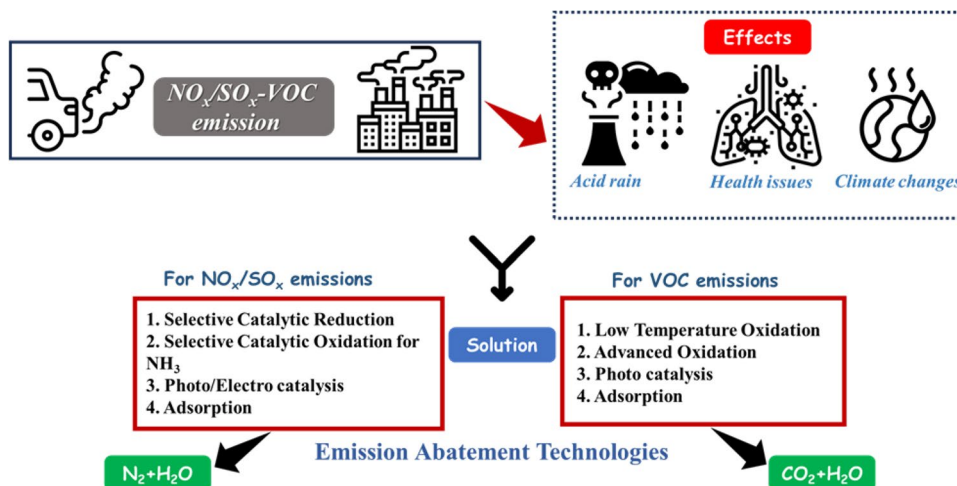
or transition metal-based catalysts (Mn, Ce, Cu, Fe, V, W) (Roy et al. 2008a, b, d; Li et al. 2017b; Liu et al. 2017; Jiang et al. 2018a; Chang et al. 2020; Zhang et al. 2021b).

Noble metal-based catalysts for SCR: Pt, Ru, Rh, Au, Pd

Noble metals like Pt, Pd, Ru, Rh, etc. are used as the catalyst for SCR. Very high conversions to NH_3 and good N_2 selectivity are possible with noble metals like Pt, Ru, Rh, and Pd. Some of the noble metal-based catalyst systems for NO_x conversion are shown in Table 2 (Sato et al. 2016), and Pt-based catalysts are also important for NO_x reduction (García Cortés et al. 2007). Another important aspect emerged is the metal-support interaction. Synergistic effect of noble metal with other metals as metal-support increases the activity (Xue et al. 2018). $Pt/La_{0.7}Sr_{0.2}Ce_{0.1}FeO_3$ catalyst can convert 87% of 2500 ppm NO at 150 °C (Costa et al. 2002). Yang et al. has shown that doping with noble metals such as Pt, Pd, Rh, Ru on MnO_x-CeO_2 matrix has increased the catalytic activity compared to undoped structure (Yang et al. 2018).

Non-noble metal-based catalysts

Non-noble metal catalysts like manganese, cerium, and vanadium are widely accepted as SCR catalysts due to its abundancy, low cost, high activity towards NO_x conversion, nitrogen selectivity, and sulfur resistance. Vanadium-based catalysts such as V_2O_5/TiO_2 and $V_2O_5/WO_3/TiO_2$ are currently commercially used SCR catalysts that operate at temperatures above 350 °C (Cha et al. 2016; Wang et al. 2018a; Yang et al. 2020; Inomata et al. 2021; Wu et al. 2021; Zhang et al. 2021a). Furthermore, details on non-noble metal catalysts are elaborated in the following sections.

Non-noble metal oxides

Non-noble metal oxides generally constitute transition metals and rare earth metals. They have gained significant attention because of their decent catalytic performance for the potential applications in SCR. Yarong et Al. prepared a series of Co_3O_4 nanoparticles inlaid in porous carbon (CoOx@PC-T) using pyrolysis of ZIF-67 in nitrogen at different temperatures. For the sample of CoOx@PC-800, greater than 80% conversion was seen in the temperature range of 150–175 °C with high nitrogen selectivity as shown in Fig. 2d–f. The greater ratio of Co^{3+}/Co^{2+}, larger surface area, and oxidizing capability of the catalyst were responsible for its performance as observed from the XPS shown in Fig. 3a–c (Bai et al. 2019). Haoxi et al. (Jiang et al. 2018b) synthesized manganese-based catalysts by a solvo-thermal method with several capping agents of PVP, P123, HAc, and CTAB to expose crystal facets of α-MnO_2. MnO_2-PVP sample with exposed (200) crystalline facets showed 100% NO conversion at 200 °C which was better than other samples. These samples also had adsorption capabilities among which MnO_2-PVP had the highest adsorption capacity. The (200) crystalline facet has maximum exposed acid sites for MnO_2-PVP, and it helped the reactant leading to maximum conversion at 200 °C.

Ole et al. (Bjørkedal et al. 2022) used zirconia as support and developed Cu/ZrO_2 by sol–gel method with different loading amounts of Cu (3%, 6%, 15%) which showed promising SCR performance, providing 75% NO conversion at 150 °C for 6 wt.% catalyst. Even though increase in copper loading (15%) increased the SCR activity at 150 °C, it was found to undergone sintering above 350 °C and showed poor selectivity. Therefore, 6% Cu on ZrO_2 is found to be better catalyst among the others.

Table 3 lists the variety of other non-noble metals used for the NO_x conversion and further emphasis on the role of

Table 2 Noble metal-based catalyst for NO_x conversion and N_2 selectivity

Noble metal catalyst	Synthesis method	Conversion	Conditions	Remarks	Ref
(Rh, Ru, Pt, Pd) doped MnO_x-CeO_2/graphene catalyst	Hydrothermal method	97.9%	100 °C 500 ppm NO, 500 ppm NH_3, 0 to 200 ppm SO_2, 0 to 5 vol% H_2O, 5 vol% O_2, and balance N_2, with a gas hourly space velocity (GHSV) of 24,000 h^{-1}	Noble metals increased synergistic effect of dopant and CeO_2	(Yang et al. 2018)
Pd_xRu_{1-x} NP	Chemical reduction method using Pd and Ru precursors	100%	200 °C 1161 ppm NO, 5750 ppm CO, 467 ppm C_3H_6, 5050 ppm O_2, 1760 ppm H_2, 12.5% CO_2, balance He, total flow rate-200 mL min^{-1} Space velocity-60,000 h^{-1}	Atom level mixing enhanced the activity	(Sato et al. 2016)
Cr-Pt/ZSM-35	Wet incipient impregnation	95%	80–300 °C 1000 ppmv NO, 5000 ppmv H_2, 6.7 vol% O_2	Cr promoted the formation of NH_4^+ species to increase activity	(Yu et al. 2010)
Pt/Beta	Hydrothermal	90%	30–90 °C, 1000 ppmv NO, 1000 ppmv H_2, 4 vol% O_2	SO_2 resistance for catalysts promoted with Ce	(García Cortés et al. 2007)
Pt/WO_3/ZrO_2	Wet impregnation	~100%	25–500 °C 2000 ppmv H_2, 5 vol% O_2	Rate depended on OH species formation	(Hahn et al. 2015)
Pt/MIL-96(Al)	Hydrothermal	~100%	20–90 °C, 1000 ppmv NO, 2000 ppmv H_2, 5 vol% O_2	Synergistic of Pt particles and MIL-96 increased the efficiency	(Xue et al. 2018)
Pt/Ti-MCM-41	Wet impregnation	90%	50–300 °C 1000 ppmv NO, 5000 ppmv H_2, 6.7 vol% O_2	Promotional effect of Ti happens on anatase phase	(Li et al. 2010)
Pt/$La_{0.7}Sr_{0.2}Ce_{0.1}FeO_3$	Wet impregnation	83%	150 °C, 0.25%-NO, 1%-H_2, 5%-O_2, balance He, WHSV-40,000 mL g^{-1} h^{-1} (GHSV = 80,000 h^{-1})	20 h stability at 140 °C on the introduction of 5% H_2O	(Costa et al. 2002)

mono-metallic and bi-metallic non-noble catalysts for the NOx reduction are briefly showcased.

Non-noble metal based bimetallic catalysts

Bimetallic catalysts are combination of two different metals that exhibits several new and improved catalytic properties. For instance, Liu et al. (2020b) prepared Sm-Mn/TiO_2 by modifying Mn/TiO_2 by Samarium using ultrasonic impregnation method which improved the surface dispersion of active metal cation and Mn/TiO_2 were also prepared for comparison. Mn/TiO_2 showed best catalytic activity with optimum Mn loading of 20% showing only 52% NO_x conversion at 120 °C whereas 10 wt.% Sm modified Mn/TiO_2 showed best low-temperature catalytic activity. The optimal interaction between Mn and Sm species was achieved with 10 wt.% Sm and 20 wt.% Mn loading forming 20Mn-10Sm/TiO_2 which exhibited greater than 80% conversion in 110 − 250 °C. Similarly, Liu et al. (2020a) used urea instead of ammonia as a reductant and binary catalyst Cu-Mn/NUAC and Cu-Co/NUAC were synthesized by ultrasonic-assisted impregnation method for LTU-SCR, and it was found that catalytic performance of binary catalysts was better than unary catalyst. Their study shows the synergic effect between the two metals (Cu-Co/Mn) which will enhance the catalytic properties compared to the individual metals. One hundred percent NO conversion for $Cu_{0.5}Mn_{0.5}$/NUAC was observed as the temperature increased from 50 to 80 °C due to the synergy between the oxides of active metal increases in this range. Synergistic mechanism of a catalyst involves distinct catalytic sites acting on different substrates sites to enhance the catalytic activity.
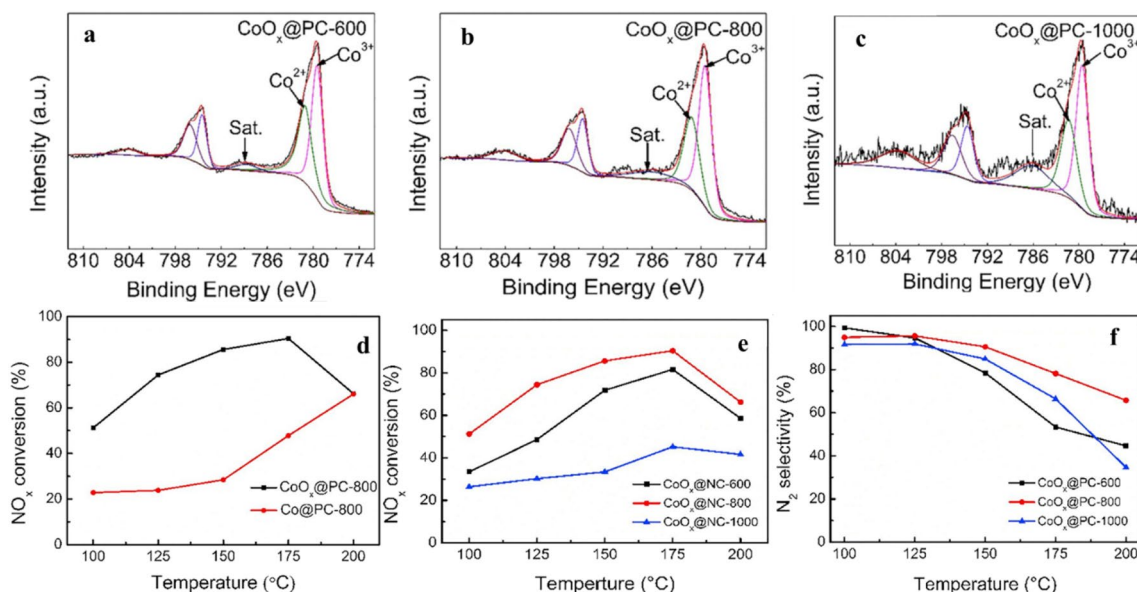
Fig. 3 XPS spectra of Co 2p in CoO$_x$@PC-600 (**a**), CoO$_x$@PC-800 (**b**), and CoO$_x$@PC-1000 (**c**). NH$_3$-SCR activity of Co@PC-800 and CoO$_x$@PC-800 (**d**). NH$_3$-SCR activity (**e**) and N$_2$ selectivity (**f**) of CoO$_x$@PC-600, CoO$_x$@PC-800, and CoO$_x$@PC-1000. Reaction conditions: [NO$_x$] = [NH$_3$] = 500 ppm, [O$_2$] = 5 vol%, Ar balance, and GHSV = 14,000 h.$^{-1}$. Reproduced from Elsevier 2019 (Bai et al. 2019)

Vanadium-based catalysts generally offer high SO$_2$ resistance, high catalytic activity due to that these materials preferred commercially (Xu et al. 2019; Kwon et al. 2021). Zhu et al. (2018) looked for the effect of niobium oxide as a promoter on V/WT (vanadium-tungsten-titanium) catalyst with different contents of dopant. Out of different contents, 6 wt.% niobium oxide (3V$_6$Nb/WTi) was found to be appropriate and catalyst deactivation was found to be negligible at around 250 °C. Similarly, the commercially used V$_2$O$_5$-WO$_3$/TiO$_2$ was mixed with several Fe$_2$O$_3$ samples (Fe(N), Fe(P), and Fe(C)). NO$_x$ conversion increased with 95% for VW/Ti + Fe at 300 °C. Addition of Fe$_2$O$_3$ inhibited the formation of ammonium sulphate thereby preventing catalyst deactivation (Zhu et al. 2018). In another study, Quanming et al. and Woojoon et al. (Cha et al. 2016; Liang et al. 2021) studied the effect of addition of cerium oxide on commercially used binary V$_2$O$_5$-WO$_3$/TiO$_2$ for NH$_3$-SCR. CeO$_2$-V$_2$O$_5$-WO$_3$/TiO$_2$ was prepared via one-step impregnation method using 0% and 3% amount of CeO$_2$. It was observed that 3Ce-3VWT could achieve 99.3% NO conversion at 160 °C. V^{4+} and V^{5+} was interchanged by the addition of 3% CeO$_2$, thereby increasing the NO$_2$/NO$_x$ ratio in flue gas that improved the low temperature catalyst.

Yunfan et al. (Xu et al. 2019) studied about its effect of V$_2$O$_5$-MoO$_3$/TiO$_2$ and V$_2$O$_5$-WO$_3$/TiO$_2$ monolithic catalysts. NO$_x$ conversion was observed to increase from 70 to 88% at 220 °C for V$_2$O$_5$-MoO$_3$/TiO$_2$ while it decreased for V$_2$O$_5$-WO$_3$/TiO$_2$. Manganese based catalysts are seen to have excellent redox ability at low temperature and have

various valence states due to that these materials are highly recommended as SCR catalysts (Fang et al. 2019; Tang et al. 2020). Specifically, the mixed metal oxides such as MnO$_x$-CeO$_2$ can reduce NO$_x$ even below 250 °C. Support materials also directly affect the catalytic performance and plays an important role in SCR. Its structure, size, and surface area have a critical role in catalytic performance (Patel and Sharma 2021). Bora Ye et al. prepared nitrogen-doped reduced graphene oxide as a support for Mn-Ce oxide catalyst (Mn-Ce/N-rGO). The catalytic activity was seen to provide 80% conversion at 200 °C. This could be achieved instead of using TiO$_2$ as support as the nanoparticles were evenly distributed without any aggregation on N-rGO which remains thermally stable at temperatures lower than 300 °C (Ye et al. 2021). Carbon monoxide can also be used as a reductant for SCR instead of NH$_3$. It has good reducing capability to convert NO into CO$_2$ and N$_2$ (Zhang et al. 2020b). Recently, metal organic frameworks (MOFs) have found to be capable for SCR due to high surface area, porosity, and synthetic tunability (Jiang et al. 2016, 2018a). Shi et al. (2021b) prepared bimetallic catalyst Ni$_{1-x}$Mn$_x$-MOF-74 with different molar ratio of Mn/(Mn + Ni) (x = 0.1, 0.2, 0.35, and 0.5) via one-pot solvothermal method which all reported higher conversion percentages in comparison to monometallic Ni-MOF-74 and Mn-MOF-74. Among them, Ni$_{0.65}$Mn$_{0.35}$-MOF-74 achieved highest conversion of nearly 100% at 175 °C and 100% nitrogen selectivity at around 200 °C. Similarly, Zhong et al. (Wang et al. 2020) prepared a novel ball-flowerlike bimetallic CoMnO$_x$-BF catalyst using

Table 3 NO$_x$ conversion by non-noble metal catalysts

Catalyst	Method of synthesis	NO conversion	Conditions	Remarks	Ref
Sm-Mn/TiO$_2$	Ultrasonic assisted impregnation	80%	110–250 °C 500 ppm of NO, 500 ppm of NH$_3$, 5 vol% of O$_2$, and balanced with N$_2$	Sm increased the redox properties enhancing oxygen concentration	(Liu et al. 2020b)
Cu-Mn/NuAC	Ultrasonic assisted impregnation	100%	50–80 °C 550 ppm of NO and 16 vol% O$_2$ balanced with N$_2$	Binary metals increase the synergistic effect	(Liu et al. 2020a)
Nb-VW/TiFe	Wetness impregnation method	95%	300 °C 500 ppm of NO, 500 ppm of NH$_3$, 3.0 vol% O$_2$, 5.0 vol% N$_2$ as balance gas	Fe$_2$O$_3$ prevent deactivation	(Zhu et al. 2018)
3Ce-3VWT	One-step impregnation	99.3%	160 °C, 500 ppm of NO and NH$_3$ and 5 vol% O$_2$, N$_2$ balanced	High NO$_2$/NO$_x$ ratio in flue gas at low temperature	(Liang et al. 2021)
V$_2$O$_5$-MoO$_3$/TiO$_2$ monoliths	Extrusion molding method	88%	220 °C 1000 ppm of NO, 5% O$_2$ and N$_2$ in balance	Separation of active site increased NH$_2$ formation thereby higher SCR activity	(Xu et al. 2019)
Mn-Ce/N-rGO	Impregnation method	80%	200 °C 500 ppm of NO$_x$, 5% of O$_2$ and 600 ppm of NH$_3$	To prevent leakage CO also used as reductant	(Ye et al. 2021)
Ni$_{1-x}$Mn$_x$-MOF-74	One-pot solvo-thermal method	100%	175 °C 500 ppm of NO, 1000 ppm of CO and N$_2$ balance	100% N$_2$ selectivity at 200 °C	(Shi et al. 2021b)
Co-MnO$_x$ -BF	Hydrothermal method	95%	150–300 °C 600 ppm of NO, 5% O$_2$, 600 ppm of NH$_3$, 5% H$_2$O and Ar as the balance gas	Good SO$_2$ resistance Stability till 36 h	(Wang et al. 2020)
CrZrO$_x$	Co-precipitation	96%	180–300 °C 500 ppm of NO, 500 ppm of NH$_3$, O$_2$ 10%, N$_2$ balance	Excellent SO$_2$ and H$_2$O resistance	(Guo et al. 2021a)
La$_{0.7}$Sr$_{0.3}$CoO$_3$	Wetness impregnation	88.5%	300–350 °C 400 ppm of NO, 1000 ppm of C$_3$H$_6$, 5 vol.% O$_2$, and the balance N$_2$	SCR-LNT coupled system is preferable to the elimination of NO$_x$ with high concentration	(Zhao et al. 2018)

hydrothermal method for NH_3-SCR. It was observed that it was SO_2 resistant and had better catalytic performance in terms of conversion (in range of 150 to 350 °C) and N_2 selectivity than $CoMnO_x$ catalyst and was also more durable catalyst to provide high NO_x conversion till 36 h. This is attributed to the large surface area of the $CoMnO_x$-BF catalyst, also the strong interaction between Mn and Co.

Non-noble metal-based tri/poly-metallic catalysts

Some dopants like Co and Ce can be used to enhance the performance of bimetallic catalysts and resistance against SO_2 deactivation (Wang et al. 2019a). Liu et al. (2019b) studied the effect Co doping onto Mn-Sm/Ti for NH_3-SCR using ultrasonic-assisted impregnation method with various amounts of doping. For 5 wt.% Co loading, 5CoMnSm/Ti achieved greater than 90% conversion at 100–200 °C having a GHSV of 60,000 h^{-1}. Qinghua et al. (Yan et al. 2018) prepared a $Cu_{0.5}Mg_{1.5}Mn_{0.5}Al_{0.5}O_x$ synthesized from layered double hydroxides via co-precipitation method. It showed high conversion ranging from 87 to 96.6% in 100–250 °C. The highest NO_x conversion was observed for $Cu_{0.5}Mg_{1.5}Mn_{0.5}Al_{0.5}O_x$ providing 96.7% conversion at 150 °C in comparison to others $Cu_{0.5}Mg_{1.5}Mn_{0.5}Al_{0.5}O_x$ (96.7%) > $Mg_2Mn_{0.5}Al_{0.5}O_x$ (93.3%) > Cu_1Mg_1-$Mn_{0.5}Al_{0.5}O_x$ (92.2%) > $Cu_{1.5}Mg_{0.5}Mn_{0.5}Al_{0.5}O_x$ (91.3%) > $Cu_2Mn_{0.5}Al_{0.5}O_x$ (91.2%). Similarly, Wei et al. (Wei et al. 2018) used co-precipitation method to synthesize a series of iron-samarium mixed oxide catalysts modified by zirconium, cobalt, and titanium. $Ti_{0.1}Sm_{0.075}Fe_{0.825}O_x$-400 sample possessed the best activity up to 95% at 150 °C and N_2 selectivity of $Ti_{0.1}Sm_{0.075}Fe_{0.825}O_x$-400 and $Zr_{0.1}Sm_{0.075}Fe_{0.825}O_x$-400 was above 95% which was higher than that of $Sm_{0.075}Fe_{0.825}O_x$-400 between 100 and 250 °C, suggesting that modification by transition metals can enhance the catalytic activity of iron-samarium mixed oxides. Tourmaline, a manganese-iron-cerium-oxide composite, plays an important role in enhancing the catalytic activity. Zhao et al. (Zhao et al. 2020a) observed the effect of tourmaline on $CeMnFeO_x$ catalyst. Manganese-iron composite catalyst and a manganese-iron-cerium composite catalyst were prepared and named as M7F3 and MFC-0.02. For 2% addition of tourmaline, NO_x conversion for MFCT-2% was 100% at 170 °C which was highest among all the other samples. Addition of tourmaline promotes the uniform distribution of layered composite materials on the surface and even small quantities of tourmaline can disperse the particles more effectively. The structure of catalysts also plays a critical role in its activity. Zhou et al. (Zhou et al. 2020) synthesized a two-dimensional MnFeCo layered double oxide (MnFeLDO, MnCo-LDO, and MnFeCo-LDO), based on the transition metal chemical compositions. Layered double oxides have large specific surface area and various active sites that enhance the activity. It was found that at 100 °C, 100% NO conversion was achieved and even at 50 °C, 86% conversion was observed. In presence of 5% H_2O vapor and 100 ppm SO_2, NO conversion was seen to be 89% and this further shows layered double oxide materials as the highly effective catalysts even under these operating conditions.

Alkali metal promoted NO_x reduction

The electro-positive nature of alkali metals as promoters are gaining interest in scientific community for NO_x reduction. Matsouka et al. have studied the un-promoted and sodium promoted Pt catalyst on supports such as Al_2O_3, CeO_2/La_2O_3 modified Al_2O_3. The study was conducted at under automobile exhaust conditions with CO, NO, C_3H_6, and O_2. Pt on Al_2O_3 support mainly has formats and acetates, leading to carbonyl species formation. But when Na is added as a promoter 100% NO reduction was at 395 °C. Konosolakiss et al. studied two different promotions separately to observe the synergy effect on de-NOx properties. Pd/Al_2O_3-TiO_2 system and K doped Pd(K)/Al_2O_3-TiO_2 system was thoroughly studied and found that K doping improves NO_x reduction (85% at 100–400 °C) and N_2 selectivity. This indicates a synergy effect in the latter catalyst. This is because Na usually strengthens the metal-NO bond and that, in turn, weakens the N–O bond due to its electro-positive nature to adsorb the electron acceptor molecule NO. This was confirmed by performing TPD over model Na on Pt (111) surface. Yentekakis et al. explored a comparative study by a promoted Pt/γ-Al_2O_3 for three reactions $C_3H_6 + NO + O_2$, $C_3H_6 + O_2$, and $NO + O_2$ at similar conditions with excess oxygen. Their studies showed how Na affecting electron-donating hydrocarbon and electron-accepting NO at lower temperatures. At Na loading of 2.6%, the NO dissociation is found to be limited with significant NO_2 formation. In another study by Consuega et al., Pt/K-γAl_2O_3/Pt was used as electrochemical catalyst for NO_x storage/reduction properties. Here, the catalytic system allows for the electrochemical storage of NO_x as potassium nitrates and simultaneously decomposes by the positively polarized film without changing the reaction atmosphere. The electro-positive nature of alkali metals supports NO decomposition and, thereby, NO_x reduction. This happens via bond strengthening of NO on alkali metal-induced metal.

Hydrocarbons/H_2 for NO_x reduction

Currently, there is a significant focus on reducing NO_x emissions using hydrocarbons or carbon monoxide, mainly by taking out gas mixtures from exhaust gases like CO. In NO_x reduction with hydrocarbon, first NO_x will be oxidizing the surface nitrates along with conversion of hydrocarbons to surface oxygenates. Further reaction between

these intermediates leads to the formation of NCO^-, CN^- species and finally forms N_2 and CO_2. Boutros et al. has studied the NO_x reduction by ethanol using Ag and Al supported mesoporous SBA-15. The first catalyst, Ag-SBA-15 showed a better catalytic activity as Ag was doped in the catalytic system efficiently because of incipient wetness impregnation method (Boutros et al. 2009). In another study by Oton et al. NO_x reduction was done by CO by using Pt, Ni, Co, Fe, or Ni nanoparticles dispersed on porous alumina. The interaction and synergy between Pt/Ni nanoparticle and the support Al_2O_3 made Pt/Al_2O_3 and $NiPt/Al_2O_3$ as better catalysts among the other. The porous nature and Lewis-acidity sites also contributed to high performance of the catalyst. According to the kinetics based on based on Eley–Rideal and Langmuir–Hinshelwood models, here Pt^0 receives an electron from NO_x (or CO) and forms PtO_x. PtO_x then adsorbs CO (than NO_x) leading to the formation of NCO intermediates on Pt sites. Further CO oxidation to CO_2, along with N_2 reduction from NO_x monodentate occurs simultaneously leaving PtO_2 for the next redox cycle (Oton et al. 2020). Seo et al. used H_2 for the reduction of NO_x and CO over $0.5Pt-2CeO_2/TiO_2/ZrO_2$ SCR catalyst at lower temperature. By the addition of ZrO_2 at 100 °C, the catalyst showed highest NO_x reduction. The presence of CO promoted water gas shift reaction which further improved NO_x reduction at 100 °C. The structural property change was because of the following: the oxygen storage capacity due to doping Pt was high, and improvement in surface acidity in presence of CO (Choong-kil 2022).

N_2O reduction

N_2O is another class of NO_x, which is a significant anthropogenic greenhouse gases and one of the major reason for ozone depletion (Zhang et al. 2019b). Thus, reduction of N_2O to N_2 is important reaction. Recently, hydrocarbons are used for the conversion of N_2O to N_2. Hevia et al. have studied Fe-ZSM-5 zeolite for the same. Different C1-C3 alkanes, alkenes, and alkynes are used as the reductant and thoroughly checked for the N_2O reduction. Alkanes showed better catalytic activity compared to alkenes, and alkynes (very less reactive) because of their reactivity with oxygen and cost. Methane and ethane were best reductant for the N_2O reaction (Hevia 2008). Similarly, Zhang et al. have explored Mans–van Krevelen mechanism on phosphotungstic acid supported single-atom catalysts for the N_2O reduction by CO. Here the CO get oxidized by the surface oxygen present in the phosphotungstic acid, and N_2O occupies the oxygen vacancy and converts to N_2 (Zhang et al. 2019b).

SCO for NH_3 emissions

Selective catalytic reduction with ammonia (NH_3-SCR) is one of the most proficient techniques for NO_x removal because of excellent removal efficiency and low maintenance cost in which NH_3 is used as a reductant. Apart from high efficiency, this technique also has some shortcomings. For instance, high NH_3/NO_x ratio and catalyst deactivation by SO_2/H_2O poisoning leads to slipping of ammonia, initiating secondary pollution (Chen et al. 2019; Nakamura et al. 2021). NH_3 emissions are harmful to both environment and human health. Excess ammonia leads to eutrophication and also contributes in creation of secondary particulate aerosols. NH_3 emissions have adverse health effects, its high exposure can result in blindness and permanent lung damage (Gheorghe and Ion 2011). The techniques used for the removal of ammonia emissions are adsorption, catalytic decomposition and selective catalytic oxidation (Cardenas et al. 2021; Chen et al. 2021b; Pinzón et al. 2021). Selective catalytic oxidation (SCO) is one of the favorable approaches which can be used in complimenting to NH_3-SCR system to convert ammonia into nitrogen directly because of high nitrogen selectivity, low cost, and excellent efficiency (Guo et al. 2019; Gao et al. 2021). Catalysts play a key role in selective catalytic oxidation of ammonia. V_2O_5-TiO_2 oxide with addition of WO_3 or MoO_3 is used as commercial catalyst for SCO of ammonia. Several noble metals based, non-noble metal based, zeolites-based catalysts are used as active catalysts for selective catalytic oxidation of ammonia (Jabłońska and Palkovits 2016; Li et al. 2017a). Different categories of SCO catalysts have been elaborated below.

Noble metal-based catalysts

Many noble metals like Pt, Pd, Rh, Ru, and Ag show high catalytic activity for selective oxidation of ammonia in terms of high NH_3 conversion and N_2 selectivity (Zhang and He 2009; Hung 2010; Hung 2012; Ma and Schneider 2020). Similarly, some transition metal oxides have gained more attention than noble-metal based catalysts due to high nitrogen selectivity (Wang et al. 2009; Zhang et al. 2017a). Wang et al. (2019b) utilized sol–gel method to synthesize RuO_2-Fe_2O_3 composite oxide catalysts with different contents of RuO_2 (0.5%, 1%, 1.5%, and 2%) for selective catalytic oxidation of ammonia and results were compared with pure Fe_2O_3. At 100 °C, pure Fe_2O_3 achieved 100% NH_3 conversion with 79% N_2 selectivity which is less in comparison to RuO_2-Fe_2O_3 composite oxide catalyst. The sample prepared with 1.5% of RuO_2 content showed best catalytic activity with 100% NH_3 conversion and 89% N_2

selectivity at 225 °C. Addition of RuO_2 had a significant effect on surface acidity of catalyst and also increased surface area. $Pt/V/TiO_2$ can even over-oxidize NH_3 to NO_x in spite of showing excellent catalytic activity at low temperatures (Kim et al. 2018; Dann et al. 2019). Therefore, support plays a vital role in activity of SCO catalysts. For instance, Liu et al. (2019a) studied the promotional effects of ethylenediamine over $Pt/SiAlO_x$ (Pt/SiAl-E) catalysts using co-impregnation method. Pt/SiAl-E showed better low-temperature activity than Pt/SiAl for NH_3-SCO. For 90% NH_3 conversion, the operating temperature was lower for Pt/SiAl-E (219 °C) in comparison to Pt/SiAl (235 °C) with almost similar nitrogen selectivity as shown in Fig. 4. Addition of ethylenediamine led to reduction of particle size which in turn led to larger surface/bulk atomic ratio increasing the active sites for SCO of ammonia.

Similarly, Sun et al. (2017a) modified Pt/ZrO_2 catalyst by the addition of W using co-impregnation method and loadings of Pt and W were 1.5 wt.% and 5 wt.%, respectively. With decrease in activation energy from 113.4 to 96.2 kJ•mol^{-1}, the light off temperature for ammonia also shifted from 284 to 249 °C with same nitrogen selectivity for both of them. Redox properties and acidic nature of the catalysts are improved due to the addition of W and it also resulted in electron transfer from W species to Pt species increasing the electron density of Pt. $Pt-WO_3/ZrO_2$ had larger number of surface acid sites which contributed to improved catalytic activity. Zhang et al. (2009) studied the role of silver species on Al_2O_3 using incipient wetness impregnation and sol–gel methods to prepare 10 wt.% Ag/Al_2O_3 catalyst and then were pre-treated by H_2. Pre-treatment of Ag/Al_2O_3 prepared by impregnation method resulted in excellent catalytic activity of 100% conversion at 160 °C. However, for fresh Ag/Al_2O_3 showed complete conversion at 220 °C. Ag^0 was concluded as the most active species at low temperatures.

Metal oxide and zeolites-based SCO catalysts

Zeolite-based materials are another class of catalysts that show promising results and have been extensively used for selective catalytic oxidation of ammonia. Their activity can be increased by addition of transition metals (e.g., Cu, Fe, Co) or noble metals (e.g., Pt/Ag/Au). The shape selectivity and high surface area often attributes to excellent SCO activity (Qi et al. 2004; Jabłońska et al. 2014; Li et al. 2017a; Rutkowska et al. 2017, 2019; Wang et al. 2021c). Therefore, many scientific studies are being done for low temperature zeolites that operate below 200 °C. With respect to low operating temperature, Wang et al. (2019c) synthesized hollow ZSM-5 encapsulating Ag particles (Ag/ZSM-5-OH) in Al_2O_3, ZSM-5 and hollow ZSM-5. For 100% NH_3 conversion, operating temperature for Ag/ZSM-5 catalyst was 110 °C. By modification of Ag nanoparticles, activation energy for Ag/ZSM-5 was found to be the lowest measuring 16.4 kJ•mol^{-1}. High content of Ag^0 species contributed to higher catalytic activity. Leaching of Ag particles was prevented via hollow structure of ZSM-5 zeolite.

Similarly, Sun et al. (2017b) modified Pt/ZSM-5 by adding Cu via co-impregnation method with loading of 1.5 wt.% of both Pt and Cu. Catalytic performance of PtCu/ZSM-5 was better than original Pt/ZSM-5. It was observed that Cu acted as promoter lowering $T_{90\%}$ temperature from 250 to 245 °C as shown in Fig. 5. It also promoted N_2 selectivity (79% at 200 °C) which was 64% for Pt/ZSM-5. It was observed that Cu species adjusted the states of Pt species thereby increasing the electron density. Dealuminated zeolites are having higher Brønsted as well as Lewis acidity, and this contributed to higher nitrogen selectivity. Metal
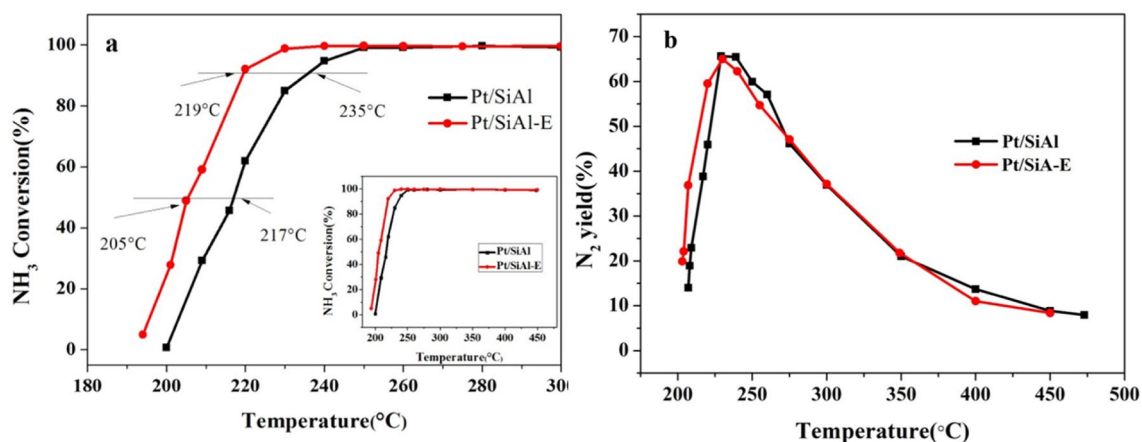

Fig. 4 **a** The NH_3 conversion of catalysts. **b** The N_2 yield of catalysts. Experimental condition: 200 ppm NH_3, 10% O_2, 8% CO_2, 5% H_2O and balance N_2. The space velocity was 100,000 h^{-1} (Liu et al. 2019a). Reproduced from Elsevier

Fig. 5 **a** NH$_3$ conversion, **b** N$_2$ selectivity, **c** Arrhenius plots of NH$_3$ oxidation, and **d** TOF profiles versus reaction temperature over the Ag/ZSM-5, Ag/Al$_2$O$_3$, and Ag/ZSM-5-OH catalyst. Reaction conditions: [NH$_3$] = 1000 ppm, [O$_2$] = 10 vol%, He balance, and GHSV = 35,000 h^{-1} (Wang et al. 2019c). Reproduced from Elsevier
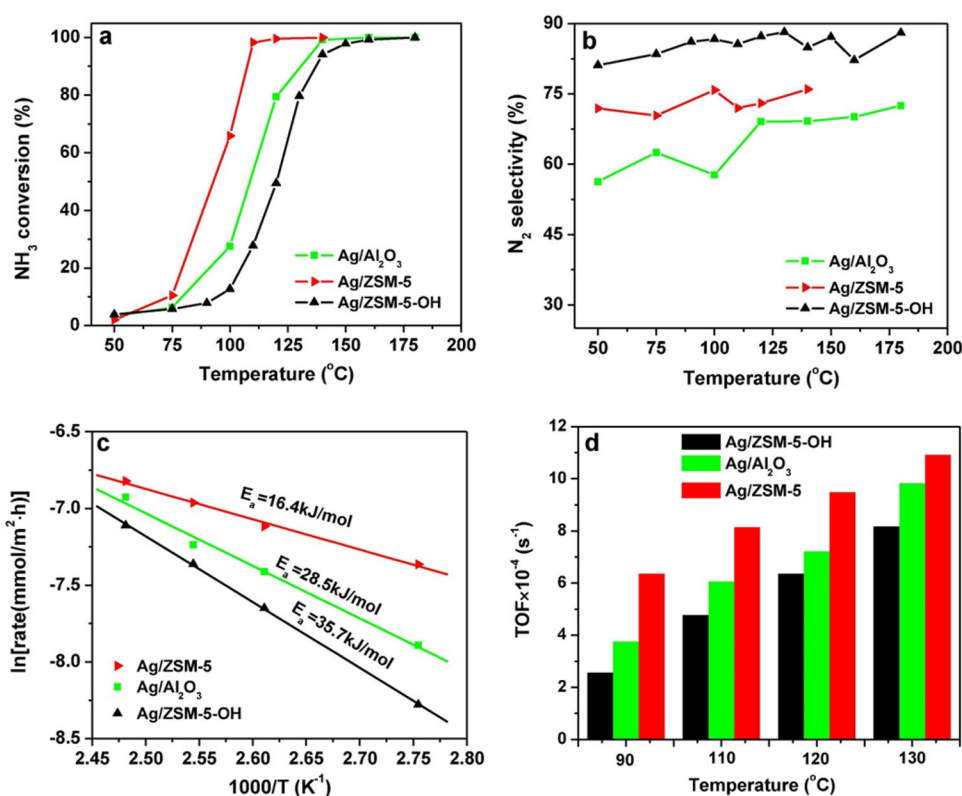
oxide-based SCO catalysts (MnO$_2$, CuO, Fe$_2$O$_3$, Co$_3$O$_4$) have higher nitrogen selectivity than noble metal-based catalysts but, they generally have lower catalytic activity. CuO/Fe$_2$O$_3$ catalysts for SCO have higher nitrogen selectivity than noble metal-based catalysts, however, majority of the catalysts offered lower catalytic activity. CuO/CeO$_2$ metal oxides can provide excellent catalytic activity as well as nitrogen selectivity (Wang et al. 2013; Zhang et al. 2017a). Further modification to the metal oxide catalysts enhances the catalytic activity. Preparation method, support and structure of catalyst plays an important role in catalytic activity and further to favorable results (Nassos et al. 2007; Jabłońska et al. 2017b, a; Wang et al. 2021a). For example, Song and Jiang (2012) prepared CuO/CNTs (carbon nanotubes) for SCO of ammonia. Nanocomposites were named as CuO/CNTs-80, CuO/CNTs-100, CuO/CNTs-120, CuO/CNTs-140, and CuO/CNTs-180. Higher the defect density of CNTs, higher catalytic activity was observed. Highest nitrogen selectivity of 98.7% was achieved on CuO/CNTs-140 with 100% NH$_3$ conversion at 189 °C. By these carbon nanotube defects, electron transfer was promoted and copper oxide was activated by these nanotubes. Similarly, Qu et al. (2015) used urea assisted hydrothermal method. MnO$_2$(UH) catalyst showed outstanding catalytic activity of 90% NH$_3$ conversion at 140 °C while 100% conversion at 170 °C which was better in contrast to MnO$_2$(H) (200 °C) and commercial MnO$_2$ (260 °C). However, some by-products like N$_2$O, NO,

and NO$_2$ were obtained that led to reduced nitrogen selectivity. Urea-assisted synthesis successfully changed the surface properties of the catalyst by imparting more adsorption sites for NH$_3$ adsorption and activation. Similarly, Duan et al. (2010) improved Cu-Mn compounds catalysts with trivalent rare earth oxide Ce$_2$O$_3$ and La$_2$O$_3$ respectively by incipient wet impregnation method. Also, comparative analysis was done for different preparation methods of 2.5%Ce-5%Cu-5%Mn/TiO$_2$ namely incipient wet impregnation, co-precipitation and sol–gel as follows. By addition of La and Ce, better distribution of Cu and Mn species was observed along with increased interaction between supporter and Cu-Mn, better oxidation ability. Selective catalytic oxidation for NH$_3$ is discussed in Table 4 in detail.

Different mechanistic pathways of NO$_x$ abatement are explained in Fig. 6. Mechanisms such as Langmuir–Hinshelwood and Eley–Rideal are explained in the schematics.

In the Langmuir–Hinshelwood mechanism, NH$_3$ adsorbs on the acid site of the catalyst to form NH$_4^+$. Further, NO will be physically adsorbed on the metallic surface. The metal with higher oxidation state undergoes reduction in order to oxidize NO to NO$_x$ species. Then, the NO$_x$ species and the adsorbed NH$_4^+$ species react to form NH$_4$NO$_x$. Further, NH$_4$NO$_x$ decomposes to N$_2$ or N$_2$O. Similarly, in Eley–Rideal mechanism, activation of NH$_3$ species by metallic site takes place forming NH$_2^-$. This NH$_2^-$ reduces NO species to N$_2$ or N$_2$O.

Table 4 SCO catalysts to control NH_3 emission

Catalyst	Conversion and selectivity	Remarks	Ref
Ag/Al$_2$O$_3$	160 °C, NH$_3$, 500 ppm; O$_2$, 10 vol.%; He as carrier; flow rate, 100 mL min^{-1}	The reaction mechanism is different above and below 160 °C. Below 160 °C, it follows in situ-selective catalytic reduction to produce N$_2$	(Zhang and He 2009)
Pt–Rh complex catalyst	95%, 600 ppm NH$_3$ in He, O$_2$=4%, temperature=350 °C, GHSV=92,000 h^{-1}	The catalyst performs well even for highly concentrated streams of NH$_3$ and may therefore lead to improvement of industrial plants	(Hung 2012)
Pt–Pd–Rh cordierite monolith	99.0%, 1000 ppm NH$_3$ in He, O$_2$=4%, RH=12%, temperature=350 °C, GHSV=92,000 h^{-1}	The catalyst showed N$_2$ selectivity of 80% with oxygen presence of 4%	(Hung 2010)
CuO-Fe$_2$O$_3$	~100%, 300 °C, 800 ppm NH$_3$, 5% O$_2$, Ar balance, flow rate 400 mL min^{-1} GHSV=60,000 h^{-1}	NO$_x$ formation during NH$_3$-SCO reaction	(Zhang et al. 2017a)
RuO$_2$-Fe$_2$O$_3$	100% conversion for NH$_3$ and 79% selectivity for N$_2$ at 300 °C, 0.08% NH$_3$, 5% O$_2$, and Ar as balance gas, total flow 400 mL min^{-1} Operating temperature range = 150−350 °C	Synergistic effect between RuO$_2$ and Fe$_2$O$_3$ was effectively improved the catalytic activity	(Wang et al. 2019b)
Pt/V/TiO$_2$	~100%, 250 °C, 200 ppm NH$_3$, 8% O$_2$, and 6% H$_2$O Flow rate=500 mL min^{-1} GHSV=60,000 h^{-1}	V increased the Brønsted acid sites, intern increased activity	(Kim et al. 2018)
EDTA modified Pt/SiAlO$_x$	~100% at 250 °C, 200 ppm NH$_3$, 10% O$_2$, 8% CO$_2$, 5%H$_2$O rest N$_2$, GHSV=100,000 h^{-1}	The properties of the catalyst enhanced with addition of EDTA	(Liu et al. 2019a)
W-Pt/ZrO$_2$	90% at 283 °C, 180 ppm NH$_3$, 8% O$_2$, and balanced with N$_2$, GHSV 100,000 h^{-1}	W modification reduced activation energy of the catalyst	(Sun et al. 2017b)
Fe-ZSM-5	99% at 400 °C, 1000 ppm NH$_3$, 2% O$_2$, and balance He. Flow rate=500 mL min^{-1} GHSV=4.6×10^5 h^{-1}	Catalytic activity trend: Fe-ZSM-5 (700) > Fe-ZSM-5 (600) > Fe-ZSM-5 (500), Fe-ZSM-5 (400), Fe-ZSM-5 (350) depending on the sublimation temperature	(Qi et al. 2004)
0.52 wt.% Pt$_{84}$Au$_{16}$/M20	90% at 144 °C, NH$_3$ (100 ppm, 50 mL min^{-1}), O$_2$ (20 mL min^{-1}), and Ar (30 mL min^{-1})	Brønsted acid sites increased the activity of the catalyst	(Wang et al. 2021c)
Micro-mesoporous Cu-ZSM-5	90% at 375 °C, 5000 ppm of NH$_3$, 25,000 ppm of O$_2$ diluted in pure helium total flow rate of 40 mL min^{-1}	Improved reducibility of Cu species is enhancing catalytic activity	(Rutkowska et al. 2017)
Mesoporous beta zeolite (Fe$_2$Cr, FeCr$_2$ and Cr$_3$ oligocations)	100% at 450–600 °C range, 5000 ppm of NH$_3$ and 25,000 ppm of O$_2$ in pure helium Flow rate of 40 mL min^{-1}	Fe increases activity and selectivity	(Rutkowska et al. 2019)
Pd-Zeolite-Y	100% at 160 °C, NH$_3$: O$_2$; H$_2$O: He=0.5:2.5:3.2:93.8 vol.% GHSV=15,400 h^{-1}	Activity was increased and N$_2$ selectivity decreased with Pd loading	(Dann et al. 2019)

Table 4 (continued)

Catalyst	Conversion and selectivity	Remarks	Ref
Ag/ZSM-5	100% at 110 °C 1000 ppm NH_3, 10 vol.% O_2, and balance He, flow rate = 100 mL min^{-1} GHSV = 35,000 h^{-1}	High activity because of Ag^0 species, Ag/ZSM-5 catalyst	(Wang et al. 2019c)
Cu into Pt/ZSM-5	90% at 250 °C, 180 ppm NH_3, 8% O_2 and balanced with N_2, GHSV-100,000 h^{-1}	Brønsted acid sites increased with Cu content	(Sun et al. 2017b)
CuO-CeO$_2$	100% at 250 °C 1000 ppm NH_3, 10 vol.% O_2, and balance He Flow rate 100 mL min^{-1} GHSV = 40,000 h^{-1}	Cu–O–Ce bond promoted lattice oxygen and thereby increased activity	(Wang et al. 2013)
Cu-Mg (Zn)-Al-(Zr) mixed metal oxides	100% at 400–500 °C NH_3; O_2; Ar = 0.5:2.5:97 vol.% Flow rate = 40 mL min^{-1} WHSV = 24,000 mL h^{-1} g^{-1}	CuO species favored activity	(Jabłońska et al. 2017b)
CuO/CNTs	100% at 230 °C 1000 ppm NH_3, 2% O_2, and balance He	CuO activated by CNTs	(Song and Jiang 2012)
MnO$_2$(UH)- urea favored	100% at 170 °C 1000 ppm NH_3, 10 vol.% O_2, balance He Flow rate 100 mL min^{-1}	Urea enhanced the surface properties and thereby activity	(Qu et al. 2015)
2.5%Ce-5%Cu-5%Mn/TiO$_2$	100% at 175 °C 500 ppm NH_3, 0.5–10% O_2, flow rate = 200 mL min^{-1} GHSV = 50,000 h^{-1}	Activity influenced by method of preparation	(Duan et al. 2010)

Fig. 6 Mechanistic pathway for NO$_x$ abatement by NH$_3$ selective catalytic oxidation and hydrocarbon selective catalytic reduction
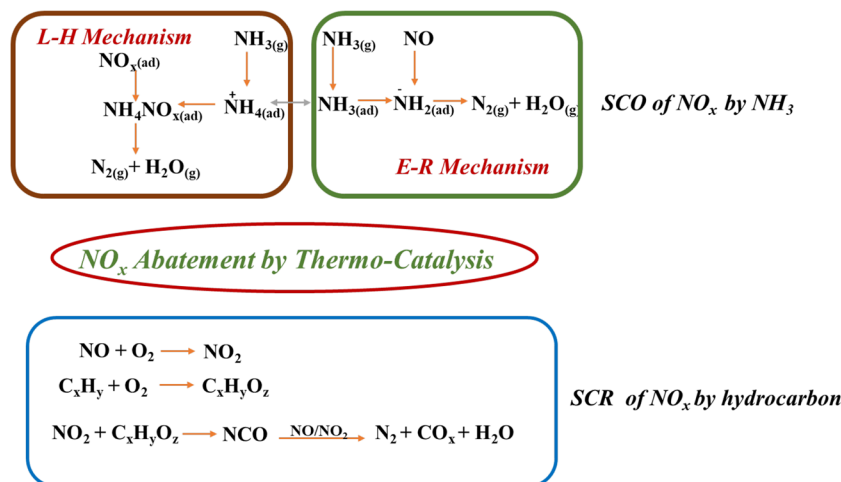
Photo/electro catalysts for the NO$_x$ removal

Numerous studies have explored the application of electro- and photocatalysis for the removal of NO$_x$, SO$_x$, and VOCs, highlighting the diverse catalyst materials and reaction mechanisms involved. Electrocatalytic reduction has been extensively studied for the removal of NO$_x$. Tan et al. (2016) explored the electrochemical reduction of NO$_x$ using various electrode materials, including metal oxides, metal alloys, and conductive polymers. The study revealed that the electrochemical reduction of NO$_x$ can effectively convert nitrogen oxides into harmless nitrogen under specific reaction conditions, presenting a viable pathway for NO$_x$ abatement One such catalyst category is using graphene-based materials. Lee et al. (2019) studied the electrocatalytic reduction of NO$_x$ using graphene-based catalysts. They reported enhanced catalytic activity and stability, suggesting graphene as a promising material for NO$_x$ removal. The utilization of visible light-responsive catalysts, such as carbon-based materials and metal–organic frameworks, was discussed as a promising avenue for improved NO$_x$ degradation. Si et al. (2021) investigated the photocatalytic reduction of NO$_x$ using TiO$_2$-based catalysts, highlighting the influence of factors such as crystalline structure and surface area on the catalytic performance. They reported high conversion rates under UV irradiation than visible light.

Conjugate polymers and their composites are renowned for their metallic conductivity and impressive physical properties subjected to doping. Foreign elements inclusion can greatly enhance the photocatalytic activity under visible light by improving the separation of charge carriers and expanding the range of light absorption. Additionally, combining conductive polymers with oxide semiconductor photocatalysts creates a synergistic effect, resulting in highly efficient photocatalytic degradation. Ajmal et al. (2023) critically evaluates the previously unexplored utilization of conjugated polymers (CPs) in combination with common inorganic semiconductors as innovative photocatalysts. The distinctive characteristics of CPs, such as conductivity, exceptional light responsiveness, effective sorption capability, superior redox charge generation, and separation abilities facilitated by a delocalized π-electron system, differentiate them from inorganic semiconductors. Ajmal et al. (2022) discussed the advancements in photocatalytic removal of three major air pollutants, namely CO$_2$, NO$_x$, and VOCs, using Conjugate Polymer based photocatalysts. Additionally, the synergistic effects observed when conjugated polymers are combined with inorganic semiconductors are comprehensively summarized. Notably, the combined system enhances charge generation and separation, potentially activating the adsorb and shuttle process, wherein conjugate polymers may play a crucial role in the sorption process. Semiconductor-based catalysts are studied for the photochemical removal of NO$_x$, such as WO$_3$ and Bi$_2$WO$_6$ (Dong et al. 2016; Zhang et al. 2019a) These catalysts facilitated the efficient photodecomposition of NO$_x$ species, offering potential solutions for NO$_x$ abatement. Photo catalysis has shown promise for the removal of SO$_x$ pollutants. The research demonstrates the potential of various catalyst materials, such as TiO$_2$-based catalysts, graphene, MOFs, and semiconductor-based catalysts, for efficient pollutant degradation. Additionally, the combination of photo and electrocatalysis has shown synergistic effects, leading to enhanced removal efficiency. However, further research is required to optimize catalyst design, improve stability, and scale up these catalytic systems for practical applications.

Adsorption techniques for the NO$_x$/SO$_x$ removal

Air pollution caused by nitrogen oxides (NO$_x$) and sulfur oxides (SO$_x$) has serious environmental and health implications. Adsorption is another effective method for the removal of these pollutants from industrial exhaust gases. Several studies have investigated the adsorption of NO$_x$, SO$_x$, and

VOCs using various adsorbents and process conditions. Mergbi et al. (2023) emphasizes the relationship between the synthesis method or surface modification of carbon materials derived from biomass waste and their effectiveness in removing organic, NO_x, SO_x, and heavy metal pollutants by photocatalysis. Surface modification of activated carbon is a technique that can enhance the presence of immobilized functional groups, leading to improved removal of NO_x from the air. Activated carbon is used for the removal of NO_x and SO_x. The primary role of activated carbon is to initially convert NO to NO_2, which can be easily adsorbed. Catalytically oxidizing NO to NO_2 could be a practical approach for removing NO_x from fuel gas, as NO_2 can be readily adsorbed.

The adsorption process for NO_x, SO_x, and VOC removal typically involves passing the gas stream through an adsorbent bed. The adsorbent materials, such as activated carbon, zeolites, and metal oxides, are selected based on their specific affinity for the target pollutants as shown in Fig. 7. The efficiency of the adsorption process depends on factors such as temperature, pressure, contact time, and adsorbent characteristics (Zhu et al. 2020; Sabzehmeidani et al. 2021; Zhu and Xu 2022). Despite the promising results, challenges persist in adsorption-based pollutant removal. Saturation of adsorbents, competition between different pollutants, and the regeneration of spent adsorbents are major hurdles that need to be addressed. The development of efficient regeneration methods and the treatment of complex gas streams are areas of ongoing research.

VOC abatement

Volatile organic compounds (VOCs) comprise organic compounds formed from burning fossil fuels, chlorination in water treatment, components of petroleum, dry cleaning agents, paint industries, etc. VOCs such as volatile benzene, toluene, ethylbenzene, and xylenes (BTEX) levels are usually higher in both industrial areas and cities (Montero-Montoya et al. 2018). Exposure to these pollutants can cause both minor and major health effects including nose, eye irritation, headache, nausea and extreme effects like kidney

or liver failure, damage to nervous system and can be even carcinogenic in some cases. VOCs have adverse effect on environment and also generates secondary pollutants. Considering the toxicity and long-term adverse effects on human health and environment, strict regulations have been set up for release of VOCs into the environment; therefore, industries need to render them harmless before releasing them into the environment (Tsimpidi et al. 2012; Manisalidis et al. 2020). Several treatment technologies for VOC abatement are being currently used such as thermal oxidation, catalytic oxidation, adsorption, photocatalysis, bio-treatments including bio trickling filters, bio-scrubbers and membrane separation (Abou Saoud et al. 2020; Zhang et al. 2020a; Cheng et al. 2021; Tian et al. 2021b; Wantz et al. 2021). Among all the possible techniques, the focus has been given to low-temperature catalytic techniques for VOC removal as it possesses low operating costs compared to other techniques.

Low-temperature catalysts for VOC oxidation

Noble metal-based catalysts

Wu et. al. (2016) synthesized three-dimensional mesoporous silica (KIT-6) was studied for toluene oxidation as shown in Fig. 8. The three-dimensionally ordered mesoporous Cr_2O_3 (meso-Cr_2O_3) was fabricated using the ultrasound-assisted strategy with KIT-6. The meso-Cr_2O_3-supported Au–Pd samples were prepared and Au and Pd loading (x) of 0.90 and 1.00 wt.% were loaded and indicated as xAu/meso-Cr_2O_3 and xPd/meso-Cr_2O_3 samples. The bimetallic 1.95Au$_1$Pd$_2$/*meso*-Cr_2O_3 sample performed exceptionally for toluene decomposition and its $T_{90\%}$ was 165 °C. Small particle size of the noble metals, high concentration of adsorbed oxygen species, low-temperature reducibility, and dispersion of noble metals contributed to excellent catalytic activity.

Similarly, Hu et al. (2018) synthesized ruthenium (Ru) nanoparticles with mass loading ranging from 1.5 to 3.2 wt.% supported on cerium dioxide (CeO_2) for application in the catalytic combustion of propane. Once Ru was loaded on the CeO_2 or Al_2O_3 support, the catalytic activities improved drastically, which clearly suggests that

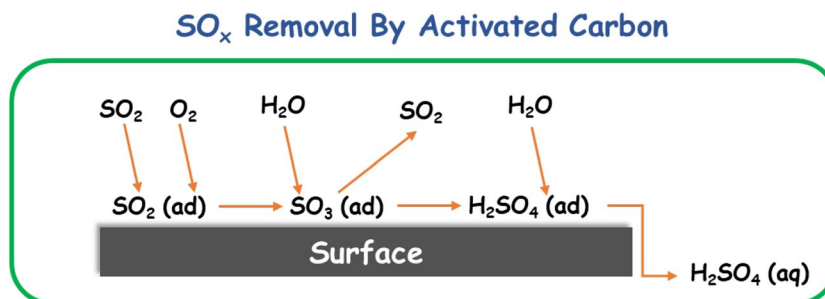**Fig. 7** Mechanistic pathway for the SO_x abatement by activated carbon

Fig. 8 **A** Toluene conversion as a function of reaction temperature of the (filled squares) *meso*-Cr_2O_3, (filled circles) $0.50Au_1Pd_2$/*meso*-Cr_2O_3, (filled triangles) $0.97Au_1Pd_2$/*meso*-Cr_2O_3, (filled diamonds) $1.95Au_1Pd_2$/*meso*-Cr_2O_3, (empty triangles) $0.90Au$/*meso*-Cr_2O_3, and (empty diamonds) $1.00Pd$/*meso*-Cr_2O_3 samples at SV = 20,000 mL g^{-1} h^{-1}. **B** Effect of SV on the catalytic activity of $1.95Au_1Pd_2$/*meso*-Cr_2O_3 for toluene oxidation (Wu et al. 2016). Reproduced from Elsevier
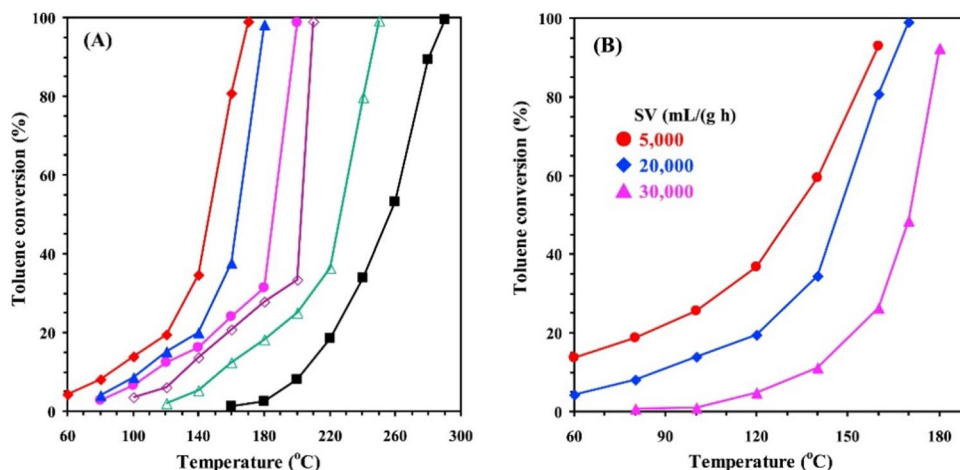
Ru has intrinsic catalytic properties for propane oxidation, which is due to the interface between Ru and CeO_2 or Al_2O_3 forms oxygen defects and attributes to strong metal support interaction, that can help in the propane oxidation. These findings confirmed that the Ru/CeO_2-X catalysts exhibited higher catalytic activities than the Ru/Al_2O_3-X catalysts in the total oxidation of propane. Also, CeO_2 support can act as a reservoir for oxygen and provide additional sites for propane adsorption. Shi et al. (2021c) prepared a series of Pt/CeO_2-TiO_2 with 0.5 wt% Pt via a modified ethylene glycol reduction method and their activity for catalytic oxidation for benzene and 1,2-dichloroethane (DCE) were tested. It was observed that Pt/CeTi-11 (where 11 represents the pH value of the synthesis solution) with the smallest average Pt particle size (1.53 nm) showed 90% conversion of benzene at 152 °C. The high performance was seen due to stronger interaction between PtO_x and CeO_2-TiO_2 support results in both the formation of more Pt^{2+} species and strong low-temperature redox properties of Pt/CeO_2-TiO_2 catalyst. Zeng et al. (2020) prepared Fe-doped Mn_3O_4 hexagonal plates with reactive (1 1 2) facet in one step and 4 nm Pd particles were loaded

on $Fe_xMn_{3-x}O_4$-HP. The methyl acetate conversion as a function of temperature is shown in Fig. 9. The stability of the catalyst was tested for 50 h and methyl acetate conversion found to be slightly decreased during the 50-h time on stream.

It was found that Fe doping increases the oxidation state of the Pd that supports the formation of highly active oxygen species in greater extent. The targeted VOC was methyl acetate and Pd/$Fe_{0.135}Mn_{2.865}O_4$ exhibited best catalytic performance of the lowest $T_{100\%}$ of 200 °C. Zhao et al. (2020b) prepared Ru/Ti_xSn_{1-x} catalysts via incipient-wetness with aqueous solution of $RuCl_3$ and co-precipitation method for catalytic oxidation of chlorobenzene and dichloromethane. As a result of the interaction between Ru and TiO_2/SnO_2, higher concentration of surface oxygen was observed. This is because of Ru–O–Ti and Ru–O-Sn interactions where they enhance strong basic surface lattice oxygen is possible and it further increase surface oxygen mobility. Moreover, the interface Ru–O-Sn has high Lewis acidity which enhances the transfer of surface oxygen to active site making suitable for dichloromethane oxidation.

Fig. 9 **a** Catalytic activity of $Fe_xMn_{3-x}O_4$-HP, Pd/Mn_3O_4-HP, and Pd/$Fe_xMn_{3-x}O_4$-HP for methyl acetate combustion. **b** Stability test of Pd/$Fe_{0.135}Mn_{2.865}O_4$-HP at 190 °C with an initial conversion of 75% (Zeng et al. 2020). Reproduced from Elsevier
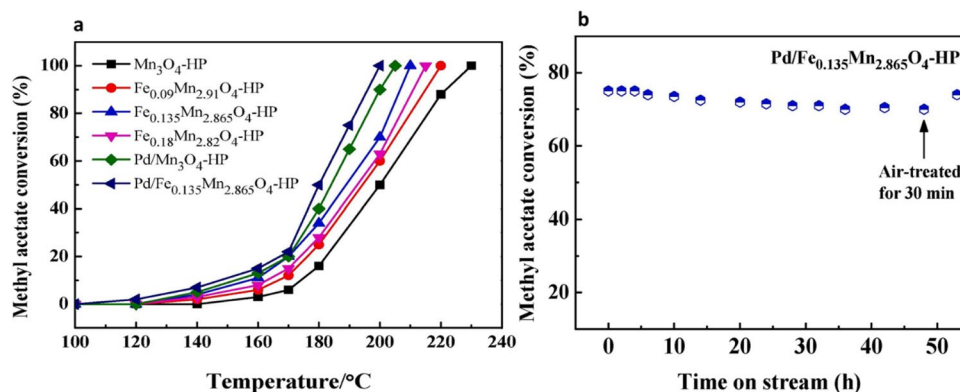
Non-noble metal-based catalysts

Similarly, Zhenxuan Zhao et al. prepared three-dimensionally ordered macro-porous $La_{0.6}Sr_{0.4}FeO_{3-\alpha}$ (LSF) for oxidation of toluene. Among the prepared LSF catalysts, LSFPEG (PEG-polyethylene glycol) has high catalytic performance for toluene combustions $T_{10\%}$, $T_{50\%}$, and $T_{90\%}$ of the LSF-PEG were 54, 225, and 280 °C, respectively. Low-temperature reducibility, high specific surface area, and high oxygen ad-species concentration of LSFPEG contributed to achieve improvement in catalytic activity.

Peng et al. (2020) performed low-temperature oxidative degradation of formaldehyde (HCHO) via novel manganese dioxide (MnO_2)/N-doped carbon nanotubes (NCNT) composites having varying MnO_2 content and the catalyst was defined as 70% MnO_2/CNTs (40% MnO_2/CNTs, 20% MnO_2/CNTs). When the temperature increased above 100 °C, the composite with the highest MnO_2 content (70% MnO_2/CNTs) showed the best activity with 100% HCHO removal efficiency at 150 °C. A complete 100% conversion of HCHO to CO_2 on 40% MnO_2/NCNT was obtained at as low as 100 °C, which was about 50 °C lower than the equivalent MnO_2/CNT catalyst. Synergy between well-formed MnO_2-CNT interfaces and strong electron transfer contributed to excellent catalytic activity. The detailed mechanism proposed for the formaldehyde oxidation is shown in Fig. 10.

Li et al. (2021a) prepared amorphous Co-Mn binary oxides with defects for catalytic oxidation of propane. Highly defective $Co_1Mn_3O_x$ showed highest catalytic activity of $T_{90\%}$ at 207 °C and high space velocity of 18,000 mL g^{-1} h^{-1}. It possesses numerous oxygen vacancy defects that weaken the Mn–O bond and improve the mobility of surface lattice oxygen which in turn leads to activation of C-H bond and helps in oxidation. Zhao et al. (2020c) synthesized monolithic Co_3O_4 and $Co_3O_4@MnO_x$ by a hydrothermal method and among the different catalysts synthesized bamboo leaf like Co_3O_4-NF-10 showed $T_{90\%}$ at 193 °C. The catalyst prepared with NH_4F as template agent and gave stronger adherence onto the Ni foam. Then, another catalyst $Co_3O_4@MnO_x$_NF was prepared by secondary hydrothermal method which showed $T_{90\%}$ at 177 °C which was 16 °C lower than Co_3O_4-NF-10. The improved performance is

Fig. 10 **a** Proposed formaldehyde oxidation mechanism on MnO_2-CNTs/NCNT. **b** Catalytic cycle of formaldehyde oxidation on MnO_2-based on DFT calculations and the oxygen molecule activation on CNT and NCNT. Where red = O, white = H, grey = C, blue = N and purple = Mn (Peng et al. 2020). Reproduced from Elsevier
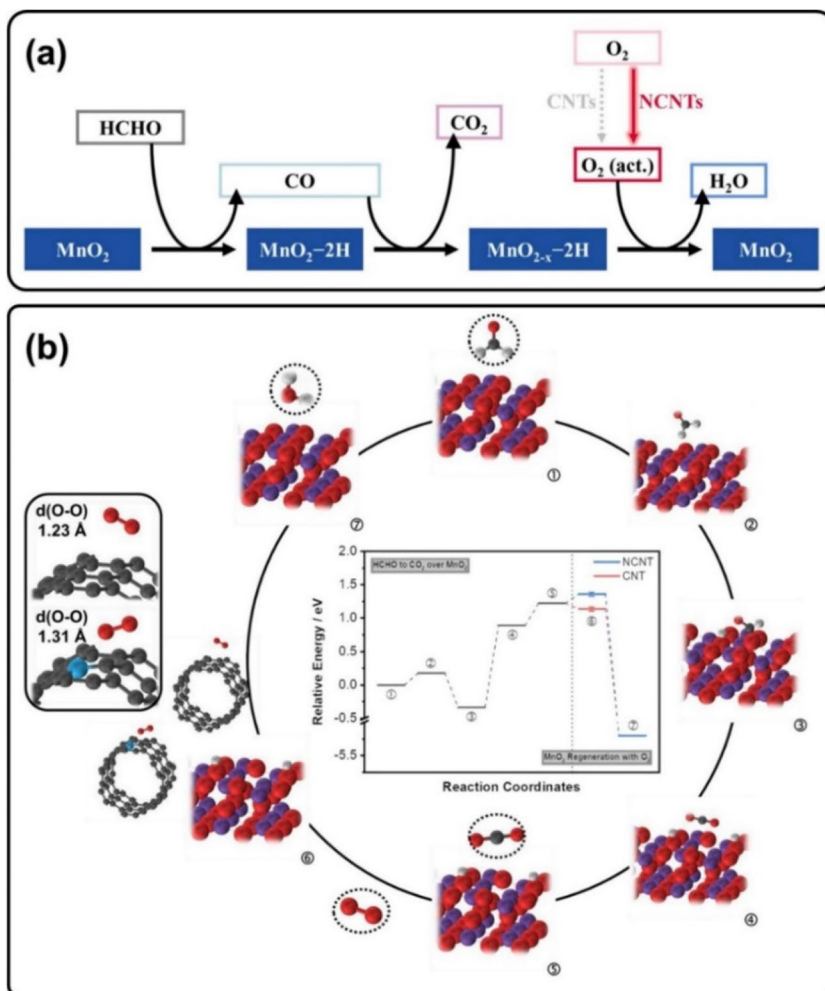
attributed to abundant Co^{3+} and increased the concentration of surface adsorbed oxygen species.

VOC removal using AOPs

VOC can be removed by using other AOPs such as photocatalysis and catalytic ozonation. Catalytic ozonation is predominantly focused by Ikhlaq et al. and Fujita et al. in presence of zeolites, TiO_2, and Al_2O_3 (Fujita et al. 2004; Ikhlaq et al. 2014). Manganese oxide-based catalysts are preferred for catalytic ozonation of VOCs and manganese addition can improve the decomposition rates of certain VOC like toluene. These metal-oxide catalysts are cost effective and have high redox potential (Xu et al. 2017; Shao et al. 2021; Gan et al. 2021).

Catalytic ozonation can degrade pollutants at lower temperature in comparison to catalytic oxidation which makes the process to be more feasible and safer for industrial use (Shao et al. 2021). In a study, Chen et al. (2020) performed catalytic ozonation of chlorobenzene over some MnO_x-based catalysts using different supports namely Al_2O_3, TiO_2, SiO_2, CeO_2, and ZrO_2. The manganese oxide-based catalysts were synthesized via an impregnation method and were tested at 120 °C. Mn/Al_2O_3 showed highest chlorobenzene conversion efficiency of 89.2% owing to its excellent textual properties, O_2 desorption, redox ability, its desirable surface adsorbed oxygen species and acidity. The other catalyst performance was in the following order: $Mn/TiO_2 > Mn/SiO_2 > Mn/CeO_2 > Mn/ZrO_2$. Another study by Amir et al. (Ikhlaq and Kasprzyk-Hordern 2017) revealed that as opposed to alumina, zeolites promoted decomposition of VOCs and catalytic ozonation of volatile organic compounds on zeolites takes a non-radical path which involves reactions of molecular ozone with pollutants adsorbed on the surface of zeolites since the presence of hydroxyl radical did not have significant effects on removal rates of VOCs.

Photocatalysis for VOC removal

Heterogenous photocatalysis in combination with catalytic ozonation also provides better results for VOC removal. The combination of these techniques overpowers the limitations of individual techniques and provides a high synergistic effect (Ebrahimi et al. 2017; Gérardin et al. 2021; Saqlain et al. 2021). But photocatalytic ozonation is difficult to scale-up therefore design optimization is required in order to make it industrially feasible. The advantage of photocatalytic route is the low operating cost as it occurs at room temperature with sun light or artificial light source that contain UV/Visible light spectrum.

The photocatalytic process involves adsorption of VOC on the surface sites of adsorbents followed by chemical reactions that convert harmful VOCs into carbon dioxide and water. As shown in Fig. 11, the semiconductors like titanium dioxide, ZnO are highly recommended which get activated by absorbing a photon via UV irradiation source which in turn leads to release of an electron from the valance band to the conduction band causing the oxidation of VOC absorbed on the surface (Zou et al. 2006; Hu et al. 2020). The photocatalysis mechanism proceeds via absorption of visible light by the catalyst, thereby creating electron hole pair in the conduction and valance band, respectively. These pairs can either recombine or can participate in the surface redox reaction. In order to maximise the charge separation and minimising the recombination many modification by doping, heterojunction and morphology enhancement taken care of (Zhao et al. 2022). Fiorenza et al. studied noble metal free co-catalyst for VOC removal. MnO_x-ZrO_2 mixed oxides
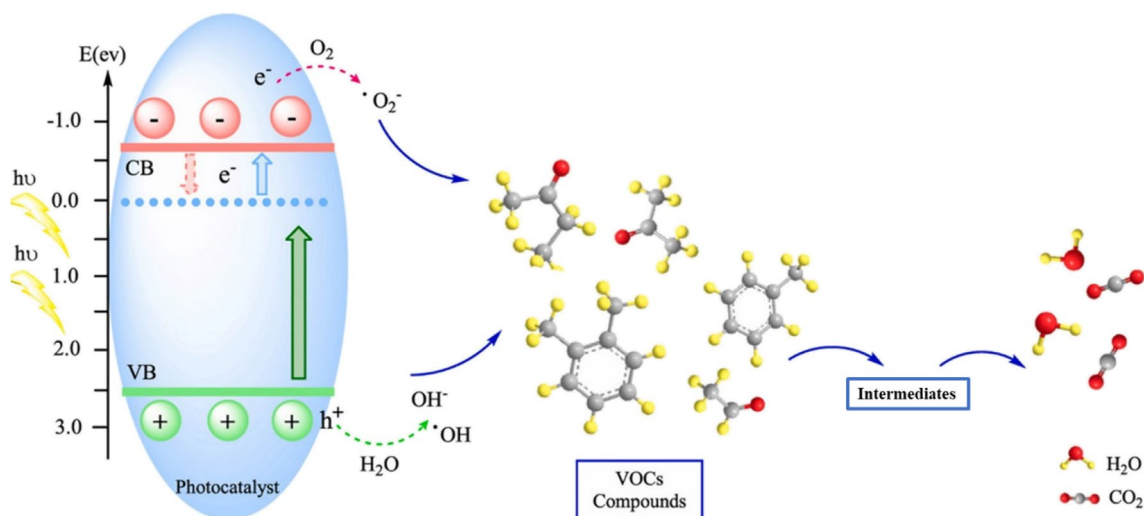

Fig. 11 Schematic of the basic mechanism of photocatalysis (Almaie et al. 2022). Reproduced from Elsevier

used for removal of toluene and ethanol in the gas phase with the multi-catalytic solar photothermal approach. Among the photocatalytic, thermo-catalytic and the photo-thermo-catalytic methods for removal of VOCs, first method has the advantage of working at room temperature and that with the MnO_x-5% ZrO_2, it reached a similar activity of the most used TiO_2-based materials, showing the importance of the material (Fiorenza et al. 2022). Similarly, Enesca et.al. worked on a titania-free heterostructure based on $CuS/SnO_2/WO_3$ material and compared with single WO_3 for the removal of formaldehyde and acetaldehyde. While WO_3 showed 41% and 52%, the $CuS/SnO_2/WO_3$ material exhibits a superior photocatalytic activity of 62.9% and 78.5% for acetaldehyde and formaldehyde respectively (Alexandru Enesca and Viorel Sisman 2022). Detailed comparison of the catalyst for VOC abatement is explained in Table 5.

Adsorbents for VOC abatement

Adsorption is a simple and cost effective regenerative method for removal of volatile organic compounds at low temperature (Zhang et al. 2017b; Ma et al. 2021a). For the industrial application of VOC removal, wide variety of materials are used as adsorbents, namely, activated carbon, CNT, zeolites, metal organic frameworks, carbon nanofibers, hyper cross-linked polymer, microporous polymer, and silica gel (Wang et al. 2018b; Ojstršek et al. 2020; Zhang et al. 2020c; Anand et al. 2021; Kutluay and Temel 2021). MOFs are known to have high adsorption capacity towards VOCs due to its peculiar properties of high specific surface area, large porous volume, and numerous metal sites which can interact with gaseous molecules of VOCs. MOFs consist of metal clusters that are connected by organic ligands and can form many structures (Britt et al. 2008; Bahri et al. 2017; Ongari et al. 2017). Therefore, metal organic frameworks make excellent adsorbents. For instance, Rui Ou et al. found that structural defects in UiO-666 can actually lead to improved performance. The modified UiO-66 by adding acetic acid (HAc) via a hydrothermal method has increased the surface area and pore volume of the initial adsorbent. The modified adsorbent UiO-66–2.0 HAc has been studied for adsorption of benzene and toluene at various HAc concentrations. The adsorbent UiO-66–1.0HAc has tuning concentration of HAc/Tac = 24, and it showed highest adsorption capacity of 367.13 mg g^{-1} for benzene which was 41.9% higher than non-defected UiO-66. When the concentration of Hac/Tac was increased to 48 molar ratios, the adsorption capacity of UiO-66–2.0Hac was achieved with the highest capture values of 410.21 mg g^{-1} of toluene at 25 °C which was 93% greater than original UiO-66. The high adsorption capacities can be attributed to addition of acetic acid which controllably modulated the number of defects by missing linkers (Ou et al. 2021). Similarly, Yang et al. carried out pyrolysis

of Zn based MOF(ZIF-8) to synthesize Zn-containing graphite carbon (Zn-GC) which targeted the adsorption of formaldehyde. The adsorption capacity of it was found to be 736 times greater than commercial activated carbon and 5.6 times that of ZSM-5 adsorbents. The adsorption capacities of Zn-GC-550, Zn-GC-650, Zn-GC-750, and Zn-GC-850 for formaldehyde adsorption were 16.67, 17.57, 13.49, and 11.32 mg g^{-1} of formaldehyde, respectively, among which Zn-GC-650 exhibited the best performance. This excellent adsorption capacity is attributed to the hierarchical porous structure of the framework which enhanced the capture of formaldehyde (having a strong affinity for formaldehyde molecules) through hydrogen bonding as the porous structure provided abundant space to pass through and hold the water vapor in the air (Yang et al. 2021a).

Kutluay (2021) modified magnetic $Fe_3O_4/AC@SiO_2$ nanoparticles with 8-hydroxyquinoline-5-sulfonic acid via the co-precipitation and sol–gel methods to form $Fe_3O_4/AC@SiO_2@8HQ5SA$ as effective adsorbent for BTX (benzene, toluene, xylene) vapors. The maximum adsorption capacities of the BTX vapours by $Fe_3O_4/AC@SiO_2@8HQ5SA$ were seen to be 555.85, 620.80, and 745.54 mg g^{-1}, respectively. After five consecutive adsorption–desorption cycle tests, $Fe_3O_4/AC@SiO_2@8HQ5SA$ maintained the reuse efficiencies of 91.92%, 91.17%, and 90.65% for the BTX vapors which makes them cost-effective (Kutluay 2021). The dynamic adsorption capacities of Fe_3O_4, Fe_3O_4/AC, $Fe_3O_4/AC@SiO_2$, and $Fe_3O_4/AC@SiO_2@8HQ5SA$ for the removal of the BTX vapors is shown in Fig. 12. Activated hydrochars derived hickory wood and peanut hull with H_3PO_4 and KOH using hydrothermal carbonization method have also improved the VOCs of acetone and cyclohexane removal efficacy. Hydrochar derived from hickory wood and peanut hull were abbreviated as HH and PH. Those modified by KOH and H_3PO_4 were abbreviated as HHK, PHK, HHP, and PHP. The VOC adsorption (acetone) of the activated hydrochars (50.57–159.66 mg g^{-1}) were greater than that of the nonactivated hydrochars (15.98–25.36 mg g^{-1}), which was mainly due to increase in surface area. The adsorption capacities for acetone on HHP and PHP were 147.77 mg g^{-1} and 113.94 mg g^{-1}, which were higher than that on HHK and PHK. After several adsorption and desorption cycles, the reusability decreased slightly which means that they can be used as effective adsorbents (Yu et al. 2020) as shown in Fig. 13.

Plata-Gryl et al. made chemical modifications to nitrated asphaltenes and used these as an active layer coated on a surface of diatomaceous earth. The AsfNitro adsorbent was prepared using the methods of coating of stationary phases onto solid support. The adsorption capacities for benzene, pyridine, and 1-nitropropane increased to 26, 12, and 8 times respectively by addition of AsfNitro. Comparing to commercial carbotrap adsorbent, twice adsorption capacity was

Table 5 Literature comparison on VOC abatement

Catalyst	Use	Conditions	Conversion	Properties	Ref
3D ordered macroporous La$_{0.6}$Sr$_{0.4}$FeO$_{3-\alpha}$	Oxidation of toluene	1000 ppm toluene + O$_2$ + N$_2$ (balance), flow rate-33.3 mL min^{-1}, toluene/O$_2$ molar ratio = 1/400, space velocity. 20,000 mL g^{-1} h^{-1}	T$_{10\%}$, T$_{50\%}$, and T$_{90\%}$~54, 225, and 280 °C	Large surface area and high oxygen concentration enhance low-temperature reducibility	(Zhao et al. 2012)
MnO$_2$/N-doped CNT	Oxidative degradation of HCHO	100 ppm HCHO and GHSV 30,000 mL h^{-1} g^{-1}	95% of HCHO (at 100 ppm) into CO$_2$ at 30 °C	Synergy of well-formed interface increased the property	(Peng et al. 2020)
Co-Mn$_3$O$_x$	Catalytic oxidation of propane	propane concentration = 0.2%; WHSV = 18,000 mL g^{-1} h^{-1}	T$_{50}$ and T$_{90}$ are 169 °C and 207 °C	O-vacancy defects weaken Mn–O bond. Surface O activate C–H bond	(Li et al. 2021a)
Monolithic Co$_3$O$_4$@MnO$_x$	Acetone oxidation	580 ppm acetone, 20 vol.% of O$_2$ and N$_2$. The space velocity-17,000 mL g^{-1} h^{-1}	T$_{50}$ = 179 °C, T$_{90}$ = 193 °C	Abundant Co^{3+} increases surface adsorbed oxygen species	(Zhao et al. 2020c)
MnO$_x$-based catalysts using different supports Al$_2$O$_3$, TiO$_2$, SiO$_2$, CeO$_2$, and ZrO$_2$	Ozonisation of chlorobenzene	Molar ratio of O$_3$/VOC:10.0, temperature: 120 °C	120 °C, Mn/Al$_2$O$_3$ showed highest CB conversion efficiency of 82.92%	Catalyst performance was in the following order: Mn/TiO$_2$>Mn/SiO$_2$>Mn/CeO$_2$>Mn/ZrO$_2$	(Chen et al. 2020)
Alumina and ZSM-5 zeolite	Ozonation of chlorinated VOCs	(Cumene, 19.1±0.5 mg/L; 1,2-dichlorobenzene, 3.5±0.3 mg/L; 1,2,4-trichlorobenzene, 0.5±0.1 mg/L) or ibuprofen (20 mg/L) or acetic acid (20 mg/L) solutions (flow rate, 15 mL/min)	In 20 °C and 30 min, Cumene~95% Ibuprofene~75% Dichloro benzene~90% Trichloro benzene~90%	ZSM-5 zeolites, as opposed to alumina, are the effective catalysts of VOCs degradation	(Ikhlaq et al. 2014)
mesoporous CuO–CeO$_2$ mixed oxides	Oxidation of benzene	Benzene = 1000 ppm, flow rate-160 mL min^{-1} GHSV = 96,000 mL g^{-1} h^{-1}	T$_{100\%}$ at 280 °C	The catalyst is richer with lattice oxygen on the surface, helps in the complete oxidation	(Hu et al. 2008)
Clay mineral (halloysite) with species of Cu, Co, Co–Cu	Oxidation of toluene	Toluene concentration of 600 ppm, total flow of 200 mL min^{-1}, 0.200 g of catalyst	T$_{90\%}$ at 308 °C	A cooperative effect of Co–Cu improved activity and hallocyte has an improved structural stability	(Carrillo and Carriazo 2015)
Octahedral molecular sieve (OMS-2) catalysts	Oxidation of C$_3$H$_6$ or CO	1% C$_3$H$_6$ (CO)/He, 20% O$_2$/He, total flow rate of 10 mL min^{-1}. Weight hourly space velocity (WHSV) – 12,000 mL g^{-1} h^{-1}	C$_3$H$_6$-T$_{50\%}$, T$_{100\%}$-110 °C, 170 °C, CO-T$_{100\%}$~200 °C for MnO (todorokite)	Accessibility of oxygen species speeds up the reaction	(Wang et al. 2021d)
Mesoporous manganese oxide catalysts	Oxidation of ethylene, propylene, toluene and their mixture	1000 ppm VOCs (ethylene, propylene and toluene or their mixture) diluted in air: gas hourly space velocity (GHSV) of 19,100 h^{-1}	T$_{99.2\%}$~310 °C	Monolithic catalyst showed better catalytic activity than powder catalyst	(Piumetti et al. 2015)

Table 5 (continued)

| Catalyst	Use	Conditions	Conversion	Properties	Ref
Transition metal doped CeO_2 catalyst	Benzene -oxidation	100 ppm benzene + 20 vol%; $O_2 + N_2$ (balance) The weight hourly space velocity WHSV-60,000 $mL·g^{-1}·h^{-1}$ Total flow rate-100 $mL·min^{-1}$	$T_{50\%}$ and $T_{90\%}$ of Ce-Mn-NF-278 and 395 °C	CeO_2 and metal oxide interface enhance oxygen mobility and reactivity	(Yang et al. 2021b)
$Pt–Pd/Al_2O_3$	Catalytic oxidation of acrylic acid derivatives	Acrylic acid-558 ppm 18,280 $m^3 h^{-1}$ Space velocity-10,000 h^{-1}	At 600 °C, catalyst without pre-treatment-90 min and pre-treated catalyst-40 min to reach steady state	It was implemented industrially because of the catalyst's high reactivity and stability	(Brummer et al. 2015)
MnO_x – HT catalyst with varying crystallinity (hard template)	Catalytic combustion benzene, toluene, xylene, and ethylbenzene	Phenyl compounds concentration-1.0 vol.%, flow rate-55 mL min^{-1}, space velocity-66,000 mL $g^{-1} h^{-1}$	T_{90} of xylene, ethylbenzene and toluene-200 °C, 205 °C, 210 °C T_{60} of benzene 225 °C	The synergy between amorphous and crystal phase provide oxygen for reaction	(Zhou et al. 2014)
$Pt/δ-Al_2O_3$ catalyst and $CuO/δ-Al_2O_3$	Methane combustion	Space velocity-1800 cm s^{-1} Methane concentration-75 ppm	0–80% conversion from 25 to 374 °C $(Pt/δ-Al_2O_3)$ 25 to 524 °C $(CuO/δ-Al_2O_3)$	Catalytic combustion showed increased reactivity in $Pt/δ-Al_2O_3$ than $CuO/δ-Al_2O_3$	(Bedi and Chauhan 2020)
$La_{1-x}Ce_xMn_{1-y}Cu_yO_3$	CH_3OH, CO and CH_4	CH_3OH oxidation-0.5% CH_3OH, 20% O_2 in He, CH_4 oxidation-0.25% CH_4, 20% O_2 in He CO oxidation-5% CO, 20% O_2, in He; flow rate-30 mL min^{-1}; space velocity-22500 h^{-1}	$T_{100\%}$ for CH_3OH, CO and CH_4-142 and 104 and 438 °C	Catalytic activity enhanced by Ce addition and decreases by Fe additions	(Levasseur and Kaliaguine 2009)
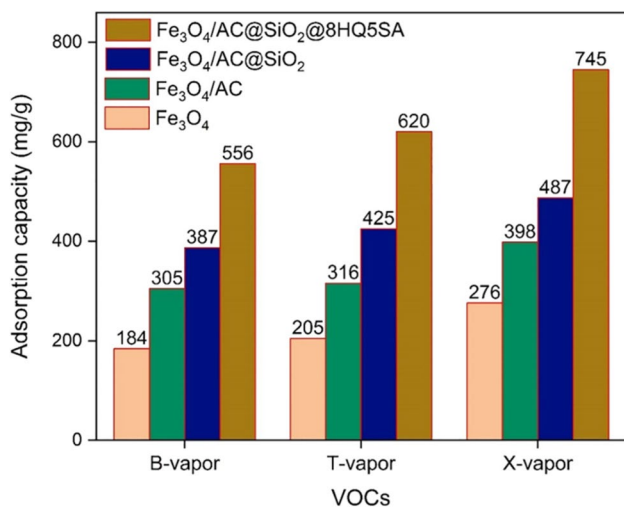
Fig. 12 The comparison of dynamic adsorption capacities of Fe_3O_4, Fe_3O_4/AC, $Fe_3O_4/AC@SiO_2$, and $Fe_3O_4/AC@SiO_2@8HQ5SA$ for the removal of the BTX vapors (Kutluay 2021). Reproduced from Elsevier

observed for benzene. However, in high humidity, there was a decrease in performance due to competitive adsorption of water molecules (Plata-Gryl et al. 2022). A schematic explaining VOC abatement mechanism on carbon surface to form CO_2 and H_2O as the final products is shown in Fig. 14. Here, L–H model is Langmuir–Hinshelwood model, where the interaction of two molecules m adsorbed at the metal surface reacts to form CO_2 and H_2O. In the second model, Eley–Rideal mechanism, reaction between gaseous O_2 and reactant adsorbed at the surface is explained. In the third mechanism, Mars-Van-Krevelen model, the catalyst surface is assumed to be an oxygen surface and thus explains the interaction of oxygen surface of the catalyst and the reactant molecules.

Catalytic converters, adsorption systems, and filtration minimize VOC emissions. These abatement procedures help meet regulatory criteria and make living situations cleaner and healthier. To design the large-scale systems, the mechanism and reaction pathway investigations are critical.
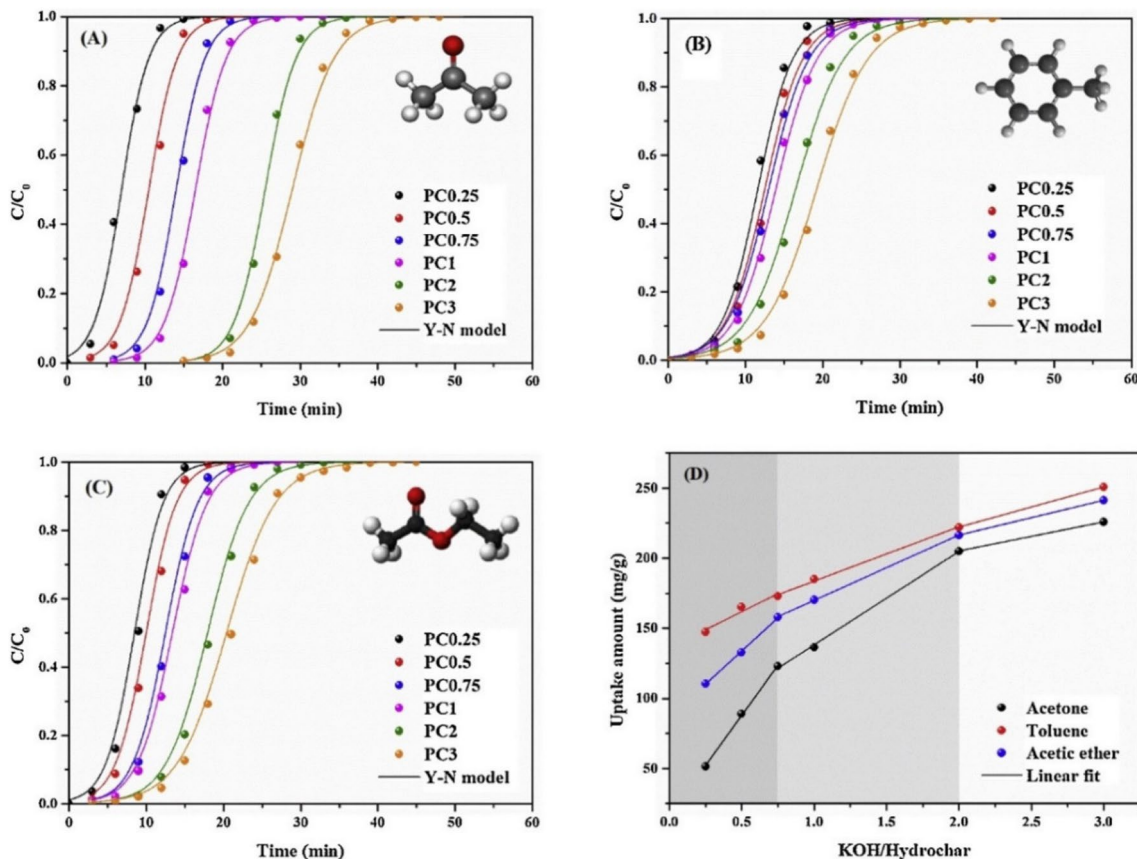

Fig. 13 Breakthrough curves of **a** acetone, **b** toluene, **c** acetic ether on PCs, and **d** adsorption capacities of PCs; 300 mg of PC at 300 K. Total adsorption flow rate-500 mL min^{-1}, with 1000 ppmv VOCs and N_2 as balance gas (Yu et al. 2020). Reproduced from Elsevier
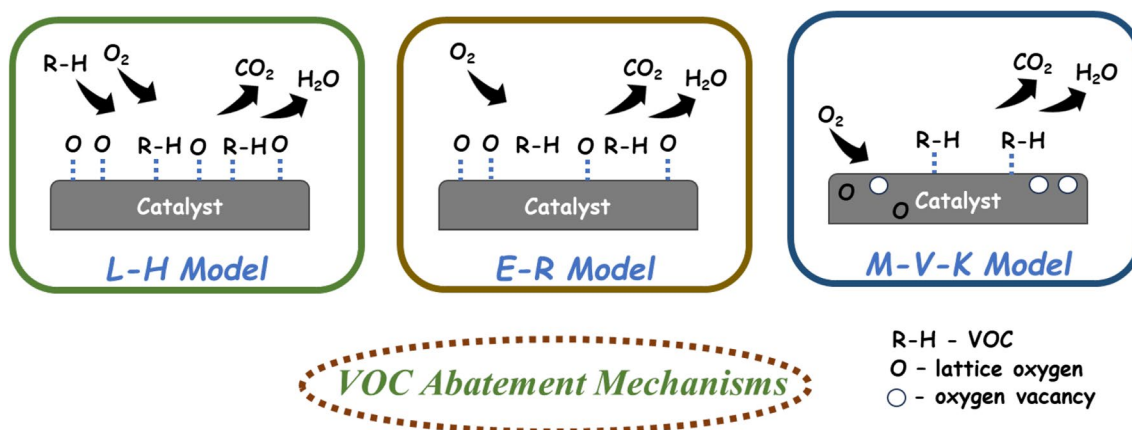
Fig. 14 Mechanistic pathway explaining the VOC abatement on carbon surface

Challenges and opportunities

Abatement technologies offer unique challenges and opportunities for the abatement of nitrogen oxides (NO_x), sulfur oxides (SO_x), and volatile organic compounds (VOCs).

Challenges

Catalyst-reactant interaction Achieving efficient catalytic conversion of NO_x, SO_x, and VOCs requires a strong interaction between the catalyst surface and the pollutants. However, the adsorption and activation of these molecules on the catalyst surface can be challenging due to their diverse chemical nature and the presence of interfering species in the reaction mixture.

Reaction kinetics The kinetics of the catalytic reactions for NO_x, SO_x, and VOC abatement can be complex. Multiple reactions, including oxidation, reduction, and acid–base chemistry, may co-occur leading to challenges in controlling reaction selectivity and optimizing conversion efficiency.

Catalyst stability Heterogeneous catalysts used for NO_x, SO_x, and VOC abatement must withstand harsh reaction conditions, such as high temperatures, corrosive environments, and exposure to water and other reactants. Maintaining catalyst stability and preventing deactivation or degradation over time is a significant challenge.

Cost and energy efficiency Implementing abatement technologies can be costly, particularly for large-scale industrial applications. Ensuring cost-effectiveness and energy efficiency in NO_x, SO_x, and VOC abatement is crucial for widespread adoption.

Opportunities

Catalyst design and development Heterogeneous catalysis offers opportunities for tailored catalyst design. Catalyst composition, structure, and active sites can be optimized to enhance catalytic activity, selectivity, and stability. Incorporating promoters, modifiers, or nano-structuring the catalyst surface can improve NO_x, SO_x, and VOC abatement performance.

NO_x abatement in hydrogen combustion engines Optimizing lean-burn combustion, employing advanced combustion techniques, utilizing exhaust gas after treatment systems like SCR and LNT (Lean NO_x Trap-NO_x adsorber to control NO_x emission from gasoline or lean burn engines), developing advanced catalyst materials, implementing engine optimization and control strategies, and establishing a robust hydrogen infrastructure are to be considered in designing efficient H_2 combustion engines. These efforts aim to minimize NO_x emissions and make hydrogen combustion engines more environmentally friendly and sustainable for transportation.

Novel catalyst materials Exploration and development of novel catalytic materials can lead to NO_x, SO_x, and VOC abatement breakthroughs. For example, advanced metal oxides, zeolites, MOFs, or hybrid catalysts combining different materials can provide higher activity, selectivity, and resistance to deactivation.

Reaction engineering Understanding and optimizing the reaction parameters and reactor design can improve catalytic performance. Strategies such as reactor configuration, flow pattern, catalyst bed geometry, and inert additives can enhance reactant/product distribution. These strategies will also facilitate better contact time with the catalyst, and

minimize mass transfer limitations, and on overall improve the abatement efficiency.

Synergistic catalytic systems Combining multiple catalysts or employing multifunctional catalysts can lead to synergistic effects and improved NO_x, SO_x, and VOC abatement performance. The overall abatement process can be enhanced by integrating complementary catalytic functions, such as oxidation and reduction.

Catalyst regeneration and recycling Developing efficient regeneration techniques or catalyst recycling methods is crucial for the economic viability of heterogeneous catalytic processes. Designing catalysts with self-cleaning properties or developing regeneration strategies, such as controlled oxidation or reduction, can extend the catalyst's lifespan and reduce the operational costs.

Process integration and scale-up Integrating heterogeneous catalytic systems into industrial processes, such as power plants, refineries, or chemical manufacturing facilities, offers opportunities for large-scale NO_x, SO_x, and VOC abatement. Catalytic technologies can be effectively implemented by optimizing process parameters, considering the overall energy efficiency, and addressing safety and economic aspects.

Innovative adsorbents and absorbents Developing novel adsorbents and absorbents with high selectivity and capacity for NO_x, SO_x, and VOC removal presents opportunities for efficient abatement. Materials such as activated carbon, zeolites, and MOFs show promise in this regard.

Conclusion and future aspects

The gradual increase in the emission of hazardous gases like NO_x, SO_x, and VOCs must be addressed on priority to safeguard the environment. Even though a large number of treatment technologies for reducing these gases are available, making these highly efficient is essential to reduce the adverse effect of the gaseous pollutant mixtures before releasing them into the atmosphere. The industries and R&D laboratories need to take radical steps in implementing technology transfer at a quicker pace. Low-temperature technologies like catalytic oxidation/reduction, non-destructive adsorption technology, redox methods like photo- and electrocatalytic ozonization are of great use with low operating cost and easily scalable for large-scale application, which are indeed required globally.

- Noble metal catalysts for NO_x reduction are preferred due to its low-temperature selective catalytic reduction,

and non-noble metals like Mn, Ce, and V were started to use because of their high conversion, sulfur resistance, and nitrogen selectivity. However, cost and availability of the materials is the paramount concern for the scalability. A few transition metal oxides, zeolites, MOFs, and their modifications also have led to achieve excellent NO_x conversion and N_2 selectivity.

- Recently flue gases containing hydrocarbon, CO are mostly highlighted for the NO_x reduction. Redox reactions such as NO_x to N_2 and hydrocarbon to CO_2 are extremely important for environment safety. The catalyst can be selected so as to have high surface area, surface acidity and oxygen storage capacity.

Oxidation of NH_3 can be considered as another important step in NO_x reduction, mainly in exhaust treatment. Four-way catalytic convertors with combination of oxidation and reduction units are getting attention nowadays for the oxidation of unreacted and excess NH_3. Thus, selective oxidation of NH_3 has its own importance.

- High conversions of NH_3 selective reduction were possible because of the increased synergic effect of non-noble metal-based bimetallic catalysts. Promoters such as NbO inhibits the catalyst deactivation even at elevated temperature.
- Zeolite-based catalysts because of their shape selectivity and high surface area attributes to excellent SCO activity. Preparation method, support, and structure of catalyst plays an important role in catalytic activity and tuning these aspects can lead to favourable results.
- Promoters such as V and W that can increase the Brønsted acidity and catalyst that has high oxygen vacancy are important for the SCO of NH_3. There are promoters like W that decreases the activation energy there by increasing the activity.

It is well known that small particle size of noble metals, high adsorbed oxygen species concentration, and low-temperature reducibility contributed to excellent catalytic activity for the VOC removal. Non-noble metal-based catalysts with large surface area, high oxygen ad-species concentration is used for VOC abatement.

- Catalytic ozonation and photocatalysis are used to overpower the limitation of VOC abatements to convert CO_2 and H_2O. Further, less-expensive adsorption technique is also efficient method to eliminate VOCs. With the help of activation, the surface nature and porosity of MOF and its derivatives can be tuned for the VOC removal.
- Inexpensive activated hydrochars can attributed to increased surface area there by increased adsorption of VOCs. By introducing linkers, desired pore tunability

can be achieved to enhance the adsorption capacity and thereby limiting the emission of pollutant gases.

Through this review, we have tried to combine the technologies for removing the gases like NO_x, SO_x, and VOC. The main application for the abatement of these gases requires in the automobile industries. Along with conventional catalytic technologies like selective catalytic reduction, advanced technologies such as advanced oxidation for the removal, adsorption, and photo-electro catalysis for the NO_x/SO_x removal have also been explored in the review. Similarly, VOC removal technologies have included low-temperature oxidation, advanced catalytic oxidation, adsorption, and other catalytic technologies. We have included how the different structures of the catalyst by modifying their surface properties have assisted in improving the catalytic properties. Dispersing active metal species like platinum, palladium, and rhodium as nanoparticles or clusters on the catalyst surface is an effective technique. This increases catalytic reaction surface area and catalyst-reactant contact, enhancing NO_x reduction efficiency. Similarly, maximizing catalyst surface area with porous or high-surface-area supports (e.g., zeolites, mesoporous materials) can boost catalytic activity. These structures increase NO_x adsorption and reaction, enhancing NO_x reduction. Likewise, functional groups or additions on the catalyst surface improve NO_x reduction selectivity and stability. Alkaline-earth metals like barium and strontium can help catalysts store and release NO_x as well as VOC species, enhancing pollutants conversion efficiency. Similarly, cerium and other transition metal oxide catalysts can alter oxidation states during catalysis. Redox behaviour helps convert NO_x as well as VOC species by transferring oxygen atoms between catalyst and reactants. Also, optimising catalyst support material affects NO_x reduction efficiency. Support acidity/basicity, thermal stability, and oxygen storage capacity can optimise NO_x reduction reaction catalytic activity and stability.

The future aspects of the abatement of gaseous pollutants involve low-cost technology. As several transition metals/carbon-based materials are abundant, relying on transition metal modified/CNT and other carbon-based supports as catalysts is a viable option from an economic viewpoint. A comprehensive understanding of the structure–activity relation, kinetic studies, and other related reaction engineering studies is yet to be explored. It is challenging to scale up the process and establish the removal in real-life applications. As discussed in the review, exploring and understanding the challenges and gaps and investigating future opportunities would be tremendous.

Declarations

Ethics approval Not applicable.

Consent to participate All the authors are consented to participate in the drafting of the review article.

Consent for publication All authors are consented to publish the review article.

Competing interests The authors declare no competing interests.

References

Abou Saoud W, Assadi AA, Kane A et al (2020) Integrated process for the removal of indoor VOCs from food industry manufacturing: elimination of butane-2,3-dione and heptan-2-one by cold plasma-photocatalysis combination. J Photochem Photobiol A Chem 386:112071. https://doi.org/10.1016/j.jphotochem.2019.112071

Ajmal Z, Haq M, ul, Naciri Y, et al (2022) Recent advancement in conjugated polymers based photocatalytic technology for air pollutants abatement: cases of CO_2, NO_x, and VOCs. Chemosphere 308:136358. https://doi.org/10.1016/j.chemosphere.2022.136358

Ajmal Z, Naciri Y, Ahmad M et al (2023) Use of conductive polymer-supported oxide-based photocatalysts for efficient VOCs & SVOCs removal in gas/liquid phase. J Environ Chem Eng 11:108935. https://doi.org/10.1016/j.jece.2022.108935

Almaie S, Vatanpour V, Rasoulifard MH, Koyuncu I (2022) Volatile organic compounds (VOCs) removal by photocatalysts: a review. Chemosphere 306:135655. https://doi.org/10.1016/J.CHEMOSPHERE.2022.135655

Anand B, Szulejko JE, Kim KH, Younis SA (2021) Proof of concept for CUK family metal-organic frameworks as environmentally-friendly adsorbents for benzene vapor. Environ Pollut 285:117491. https://doi.org/10.1016/j.envpol.2021.117491

Atkinson R, Arey J (2003) Atmospheric degradation of volatile organic compounds. Chem Rev 103:4605–4638. https://doi.org/10.1021/cr0206420

Bahri M, Haghighat F, Kazemian H, Rohani S (2017) A comparative study on metal organic frameworks for indoor environment application: adsorption evaluation. Chem Eng J 313:711–723. https://doi.org/10.1016/j.cej.2016.10.004

Bai Y, Dong J, Hou Y et al (2019) Co_3O_4@PC derived from ZIF-67 as an efficient catalyst for the selective catalytic reduction of NO_x with NH_3 at low temperature. Chem Eng J 361:703–712. https://doi.org/10.1016/j.cej.2018.12.109

Bedi U, Chauhan S (2020) Mathematical modeling of automotive catalytic converter for catalytic combustion of the volatile organic

compound (voc) methane. J Phys Conf Ser 1706:012035. https://doi.org/10.1088/1742-6596/1706/1/012035

Bjørkedal OH, Regli SK, Nuguid RJG et al (2022) One-pot synthesis of highly dispersed mesoporous Cu/ZrO$_2$ catalysts for NH$_3$-SCR. Catal Today 384–386:113–121. https://doi.org/10.1016/j.cattod.2021.05.010

Boningari T, Smirniotis PG (2016) Impact of nitrogen oxides on the environment and human health: Mn-based materials for the NO$_x$ abatement. Curr Opin Chem Eng 13:133–141. https://doi.org/10.1016/j.coche.2016.09.004

Boutros M, Trichard JM, Da Costa P (2009) Silver supported mesoporous SBA-15 as potential catalysts for SCR NO$_x$ by ethanol. Appl Catal B Environ 91:640–648. https://doi.org/10.1016/J.APCATB.2009.07.004

Britt D, Tranchemontagne D, Yaghi OM (2008) Metal-organic frameworks with high capacity and selectivity for harmful gases. Proc Nat Acad Sci USA 105:11623–11627. https://doi.org/10.1073/pnas.0804900105

Brummer V, Jecha D, Martinec J et al (2015) Impact of catalytic oxidation operating conditions on VOC and Co conversions on the Pt-Pd/Al$_2$O$_3$ catalyst. Chem Eng Trans 45:1009–1014. https://doi.org/10.3303/CET1545169

Cai X, Hu YH (2019) Advances in catalytic conversion of methane and carbon dioxide to highly valuable products. Energy Sci Eng 7:4–29. https://doi.org/10.1002/ese3.278

Cardenas C, Latifi AM, Vallières C et al (2021) Analysis of an industrial adsorption process based on ammonia chemisorption: Modeling and simulation. Comput Chem Eng 154:107474. https://doi.org/10.1016/j.compchemeng.2021.107474

Carrillo AM, Carriazo JG (2015) Cu and Co oxides supported on halloysite for the total oxidation of toluene. Appl Catal B Environ 164:443–452. https://doi.org/10.1016/J.APCATB.2014.09.027

Casagrande CA, Repette WL, Hotza D (2020) Effect of environmental conditions on degradation of NO$_x$ gases by photocatalytic nano-titania-based cement mortars after long-term hydration. J Clean Prod 274:123067. https://doi.org/10.1016/j.jclepro.2020.123067

Cha W, Ehrman SH, Jurng J (2016) CeO$_2$ added V$_2$O$_5$/TiO$_2$ catalyst prepared by chemical vapor condensation (CVC) and impregnation method for enhanced NH$_3$-SCR of NO$_x$ at low temperature. J Environ Chem Eng 4:556–563. https://doi.org/10.1016/j.jece.2015.10.033

Challagulla S, Payra S, Chakraborty C et al (2019) Understanding the role of catalytic active sites for heterogeneous photocatalytic oxidation of methanol and thermal reduction of NO$_x$. Mol Catal 476:110505. https://doi.org/10.1016/J.MCAT.2019.110505

Chang S, Harle G, Ma J, Yi J (2020) The effect of textural properties of CeO$_2$-SiO$_2$ mixed oxides on NH$_3$-SCO activity of Pt/CeO$_2$-SiO$_2$ catalyst. Appl Catal A Gen 604:117775. https://doi.org/10.1016/j.apcata.2020.117775

Chen WH, Chen CY (2020) Water gas shift reaction for hydrogen production and carbon dioxide capture: a review. Appl Energy 258:114078. https://doi.org/10.1016/J.APENERGY.2019.114078

Chen C, Cao Y, Liu S et al (2019) The catalytic properties of Cu modified attapulgite in NH$_3$–SCO and NH$_3$–SCR reactions. Appl Surf Sci 480:537–547. https://doi.org/10.1016/J.APSUSC.2019.03.024

Chen G, Wang Z, Lin F et al (2020) Comparative investigation on catalytic ozonation of VOCs in different types over supported MnOx catalysts. J Hazard Mater 391:122218. https://doi.org/10.1016/j.jhazmat.2020.122218

Chen R, Zhang T, Guo Y et al (2021a) Recent advances in simultaneous removal of SO$_2$ and NO$_x$ from exhaust gases: removal process, mechanism and kinetics. Chem Eng J 420:127588. https://doi.org/10.1016/j.cej.2020.127588

Chen Y, Chen X, Ma X et al (2021b) Selective catalytic oxidation of ammonia over AMn$_2$O$_5$ (A = Sm, Y, Gd) and reaction selectivity promotion through Nb decoration. J Catal 402:10–21. https://doi.org/10.1016/j.jcat.2021.07.027

Cheng HH, Lu IC, Huang PW et al (2021) Biological treatment of volatile organic compounds (VOCs)-containing wastewaters from wet scrubbers in semiconductor industry. Chemosphere 282:131137. https://doi.org/10.1016/j.chemosphere.2021.131137

Choong-kil, (2022) Improvement of NO$_x$ and CO reduction performance at low temperature of H$_2$-SCR catalyst. Int J Automot Technol 23:1509–1515. https://doi.org/10.1007/s12239

Costa CN, Savva PG, Andronikou C et al (2002) An investigation of the NO/H$_2$/O$_2$ (Lean De-NO$_x$) reaction on a highly active and selective Pt/La$_{0.7}$Sr$_{0.2}$Ce$_{0.1}$FeO$_3$ catalyst at low temperatures. J Catal 209:456–471. https://doi.org/10.1006/JCAT.2002.3645

Dann EK, Gibson EK, Blackmore RH et al (2019) (2019) Structural selectivity of supported Pd nanoparticles for catalytic NH$_3$ oxidation resolved using combined operando spectroscopy. Nat Catal 22(2):157–163. https://doi.org/10.1038/s41929-018-0213-3

Dong P, Xu N, Xu Y, Wang X (2016) A study of Pt/WO$_3$-carrier catalysts for photocatalytic purification of NO gas. Catal Commun 84:142–146. https://doi.org/10.1016/j.catcom.2016.06.027

Duan K, Tang X, Yi H et al (2010) Rare earth oxide modified Cu-Mn compounds supported on TiO$_2$ catalysts for low temperature selective catalytic oxidation of ammonia and in lean oxygen. J Rare Earths 28:338–342. https://doi.org/10.1016/S1002-0721(10)60277-3

Ebrahimi H, Shahna FG, Bahrami A et al (2017) Photocatalytic degradation of volatile chlorinated organic compounds with ozone addition. Arch Environ Prot 43:65–72. https://doi.org/10.1515/aep-2017-0006

Enesca A, Sisman V (2022) Indoor air photocatalytic decontamination by UV–Vis activated CuS/SnO$_2$/WO$_3$ heterostructure. Catalysts 12:728. https://doi.org/10.3390/catal12070728

Fang D, Li D, He F et al (2019) Experimental and DFT study of the adsorption and activation of NH$_3$ and NO on Mn-based spinels supported on TiO$_2$ catalysts for SCR of NO$_x$. Comput Mater Sci 160:374–381. https://doi.org/10.1016/J.COMMATSCI.2019.01.025

Fiorenza R, Farina RA, Malannata EM et al (2022) VOCs photo-thermo-catalytic removal on MnO$_x$-ZrO$_2$ catalysts. Catalysts 12:1–17. https://doi.org/10.3390/CATAL12010085

Fujita H, Izumi J, Sagehashi M et al (2004) Decomposition of trichloroethene on ozone-adsorbed high silica zeolites. Water Res 38:166–172. https://doi.org/10.1016/S0043-1354(03)00392-0

Gan Q, Fu M, Zhang Y et al (2021) Synergistic catalytic ozonation of toluene with manganese and cerium varies at low temperature. Chinese Chem Lett 33:2726–2730. https://doi.org/10.1016/J.CCLET.2021.09.006

Gao F, Liu Y, Sani Z et al (2021) Advances in selective catalytic oxidation of ammonia (NH$_3$-SCO) to dinitrogen in excess oxygen: a review on typical catalysts, catalytic performances and reaction mechanisms. J Environ Chem Eng 9:104575. https://doi.org/10.1016/j.jece.2020.104575

García Cortés JM, Illán Gómez MJ, Martínez S, de Lecea C (2007) The selective reduction of NO$_x$ with propene on Pt-beta catalyst: a transient study. Appl Catal B Environ 74:313–323. https://doi.org/10.1016/J.APCATB.2007.03.004

Gérardin F, Cloteaux A, Simard J, Favre É (2021) A photodriven energy efficient membrane process for trace VOC removal from air: first step to a smart approach. Chem Eng J 419:129566. https://doi.org/10.1016/j.cej.2021.129566

Gheorghe IF, Ion B (2011) The effects of air pollutants on vegetation and the role of vegetation in reducing atmospheric pollution. Impact Air Pollut Heal Econ Environ Agric Sources. https://doi.org/10.5772/17660

Gokhale AA, Dumesic JA, Mavrikakis M (2008) On the mechanism of low-temperature water gas shift reaction on copper. J Am Chem Soc 130:1402–1414. https://doi.org/10.1021/ja0768237

Guo J, Peng Y, Zhang Y et al (2019) Comparison of NH$_3$-SCO performance over CuO$_x$/H-SSZ-13 and CuO$_x$/H-SAPO-34 catalysts. Appl Catal A Gen 585:117–119. https://doi.org/10.1016/j.apcata.2019.117119

Guo M, Liu Q, Liu C et al (2021a) Rational design of novel CrZrO$_x$ catalysts for efficient low temperature SCR of NO$_x$. Chem Eng J 413:127554. https://doi.org/10.1016/J.CEJ.2020.127554

Guo Y, Wen M, Li G, An T (2021b) Recent advances in VOC elimination by catalytic oxidation technology onto various nano-particles catalysts: a critical review. Appl Catal B Environ 281:119447. https://doi.org/10.1016/j.apcatb.2020.119447

Guo L, Meng F, Zeng Y et al (2020) Catalytic ozonation of NO$_x$ into HNO$_3$ with low concentration ozone over MnO$_x$-CeO$_2$/TiO$_2$: two-phase synergistic effect of TiO$_2$. Mol Catal 493:111095. https://doi.org/10.1016/j.mcat.2020.111095

Hahn C, Endisch M, Schott FJP, Kureti S (2015) Kinetic modelling of the NO$_x$ reduction by H$_2$ on Pt/WO$_3$/ZrO$_2$ catalyst in excess of O$_2$. Appl Catal B Environ 168–169:429–440. https://doi.org/10.1016/J.APCATB.2014.12.033

He C, Cheng J, Zhang X et al (2019) Recent advances in the catalytic oxidation of volatile organic compounds: a review based on pollutant sorts and sources. Chem Rev 119:4471–4568. https://doi.org/10.1021/acs.chemrev.8b00408

Hevia MAG (2008) Optimal hydrocarbon selection for catalytic N$_2$O reduction over. Environ Sci Technol 42:8896–8900

Highlights P (1978) The economic consequences of air pollution. Environ Pollut 15:313. https://doi.org/10.1016/0013-9327(78)90018-6

Hu C, Zhu Q, Jiang Z et al (2008) Preparation and formation mechanism of mesoporous CuO–CeO$_2$ mixed oxides with excellent catalytic performance for removal of VOCs. Microporous Mesoporous Mater 113:427–434. https://doi.org/10.1016/J.MICROMESO.2007.11.043

Hu Z, Wang Z, Guo Y et al (2018) Total oxidation of propane over a Ru/CeO$_2$ catalyst at low temperature. Environ Sci Technol 52:9531–9541. https://doi.org/10.1021/ACS.EST.8B03448

Hu X, Li C, Sun Z et al (2020) Enhanced photocatalytic removal of indoor formaldehyde by ternary heterogeneous BiOCl/TiO$_2$/sepiolite composite under solar and visible light. Build Environ 168:106481. https://doi.org/10.1016/j.buildenv.2019.106481

Hung CM (2010) Characterization and performance of Pt-Pd-Rh cordierite monolith catalyst for selectivity catalytic oxidation of ammonia. J Hazard Mater 180:561–565. https://doi.org/10.1016/j.jhazmat.2010.04.070

Hung C-M (2012) Application of Pt-Rh complex catalyst: feasibility study on the removal of gaseous ammonia. Int J Phys Sci 7:2166–2173. https://doi.org/10.5897/ijps12.024

Ikhlaq A, Kasprzyk-Hordern B (2017) Catalytic ozonation of chlorinated VOCs on ZSM-5 zeolites and alumina: Formation of chlorides. Appl Catal B Environ 200:274–282. https://doi.org/10.1016/j.apcatb.2016.07.019

Ikhlaq A, Brown DR, Kasprzyk-Hordern B (2014) Catalytic ozonation for the removal of organic contaminants in water on ZSM-5 zeolites. Appl Catal B Environ 154–155:110–122. https://doi.org/10.1016/j.apcatb.2014.02.010

Inomata Y, Hata S, Kiyonaga E et al (2021) Synthesis of bulk vanadium oxide with a large surface area using organic acids and its low-temperature NH$_3$-SCR activity. Catal Today 376:188–196. https://doi.org/10.1016/j.cattod.2020.06.041

Jabłońska M, Palkovits R (2016) Copper based catalysts for the selective ammonia oxidation into nitrogen and water vapour-Recent trends and open challenges. Appl Catal B Environ 181:332–351. https://doi.org/10.1016/j.apcatb.2015.07.017

Jabłońska M, Król A, Kukulska-Zajac E et al (2014) Zeolite y modified with palladium as effective catalyst for selective catalytic oxidation of ammonia to nitrogen. J Catal 316:36–46. https://doi.org/10.1016/j.jcat.2014.04.022

Jabłońska M, Ciptonugroho W, Góra-Marek K et al (2017a) Preparation, characterization and catalytic performance of Ag-modified mesoporous TiO$_2$ in low-temperature selective ammonia oxidation into nitrogen and water vapour. Microporous Mesoporous Mater 245:31–44. https://doi.org/10.1016/j.micromeso.2017.02.070

Jabłońska M, Nocuń M, Gołąbek K, Palkovits R (2017b) Effect of preparation procedures on catalytic activity and selectivity of copper-based mixed oxides in selective catalytic oxidation of ammonia into nitrogen and water vapour. Appl Surf Sci 423:498–508. https://doi.org/10.1016/j.apsusc.2017.06.144

Jiang R, Shan H, Li C, Yang C (2011) Preparation and characterization of Mn/MgAlFe as transfer catalyst for SO$_x$ abatement. J Nat Gas Chem 20:191–197. https://doi.org/10.1016/S1003-9953(10)60171-5

Jiang Z, Jones DBA, Worden HM, Henze DK (2015) Sensitivity of top-down CO source estimates to the modeled vertical structure in atmospheric CO. Atmos Chem Phys 15:1521–1537. https://doi.org/10.5194/acp-15-1521-2015

Jiang H, Wang C, Wang H, Zhang M (2016) Synthesis of highly efficient MnO$_x$ catalyst for low-temperature NH$_3$-SCR prepared from Mn-MOF-74 template. Mater Lett 168:17–19. https://doi.org/10.1016/j.matlet.2015.12.150

Jiang H, Niu Y, Wang Q et al (2018a) Single-phase SO$_2$-resistant to poisoning Co/Mn-MOF-74 catalysts for NH$_3$-SCR. Catal Commun 113:46–50. https://doi.org/10.1016/j.catcom.2018.05.017

Jiang H, Wang Y, Zhou J et al (2018b) Morphology control of manganese-based catalysts for low-temperature selective catalytic reduction of NO$_x$. Mater Lett 233:250–253. https://doi.org/10.1016/j.matlet.2018.09.004

Jurado L, Papaefthimiou V, Thomas S, Roger AC (2021) Low temperature toluene and phenol abatement as tar model molecules over Ni-based catalysts: influence of the support and the synthesis method. Appl Catal B Environ 297:120479. https://doi.org/10.1016/j.apcatb.2021.120479

Kampa M, Castanas E (2008) Human health effects of air pollution. Environ Pollut 151:362–367. https://doi.org/10.1016/j.envpol.2007.06.012

Kathiraser Y, Oemar U, Saw ET et al (2015) Kinetic and mechanistic aspects for CO$_2$ reforming of methane over Ni based catalysts. Chem Eng J 278:62–78. https://doi.org/10.1016/j.cej.2014.11.143

Kim GJ, Kwon DW, Shin JH et al (2018) Influence of the addition of vanadium to Pt/TiO$_2$ catalyst on the selective catalytic oxidation of NH$_3$ to N$_2$. Environ Technol 40:2588–2600. https://doi.org/10.1080/09593330.20181554004

Kutluay S (2021) Excellent adsorptive performance of novel magnetic nano-adsorbent functionalized with 8-hydroxyquinoline-5-sulfonic acid for the removal of volatile organic compounds (BTX) vapors. Fuel 287:119691. https://doi.org/10.1016/j.fuel.2020.119691

Kutluay S, Temel F (2021) Silica gel based new adsorbent having enhanced VOC dynamic adsorption/desorption performance. Colloids Surfaces A Physicochem Eng Asp 609:125848. https://doi.org/10.1016/j.colsurfa.2020.125848

Kwon DW, Kim DH, Lee S et al (2021) A dual catalytic strategy by the nature of the functionalization effect as well as active species on vanadium-based catalyst for enhanced low temperature SCR. Appl Catal B Environ 289:120032. https://doi.org/10.1016/j.apcatb.2021.120032

Lee JC, Gopalan AI, Sai-Anand G et al (2019) Preparation of visible light photocatalytic graphene embedded rutile titanium(IV)

oxide composite nanowires and enhanced NO_x removal. Catalysts 9:170. https://doi.org/10.3390/catal9020170

Levasseur B, Kaliaguine S (2009) Effects of iron and cerium in $La_{1-y}Ce_yCo_{1-x}Fe_xO_3$ perovskites as catalysts for VOC oxidation. Appl Catal B Environ 88:305–314. https://doi.org/10.1016/J.APCATB.2008.11.007

Li L, Wu P, Yu Q et al (2010) Low temperature H_2-SCR over platinum catalysts supported on Ti-containing MCM-41. Appl Catal B Environ 94:254–262. https://doi.org/10.1016/J.APCATB.2009.11.016

Li P, Zhang R, Liu N, Royer S (2017a) Efficiency of Cu and Pd substitution in Fe-based perovskites to promote N_2 formation during NH_3 selective catalytic oxidation (NH_3-SCO). Appl Catal B Environ 203:174–188. https://doi.org/10.1016/j.apcatb.2016.10.021

Li X, Li X, Yang RT et al (2017b) The poisoning effects of calcium on V_2O_5-WO_3/TiO_2 catalyst for the SCR reaction: comparison of different forms of calcium. Mol Catal 434:16–24. https://doi.org/10.1016/j.mcat.2017.01.010

Li S, Song L, Zhan Z et al (2021b) Redox and acid properties of MnV_2O_x/TiO_2 catalysts synthesized by assistance of microwave for NO selective catalytic reduction by ammonia. Chem Eng J Adv 8:100156. https://doi.org/10.1016/j.ceja.2021.100156

Li Z, Jin Y, Chen T et al (2021c) Trimethylchlorosilane modified activated carbon for the adsorption of VOCs at high humidity. Sep Purif Technol 272:118659. https://doi.org/10.1016/j.seppur.2021.118659

Li G, Li N, Sun Y et al (2021a) Efficient defect engineering in Co-Mn binary oxides for low-temperature propane oxidation. Appl Catal B Environ 282:119512. https://doi.org/10.1016/j.apcatb.2020.119512

Li S, Lin Y, Liu G, Shi C (2023) Research status of volatile organic compound (VOC) removal technology and prospect of new strategies: a review. Environ Sci Process Impacts 25:727–740. https://doi.org/10.1039/d2em00436d

Liang Q, Li J, Yue T (2021) Promotional effect of CeO_2 on low-temperature selective catalytic reduction of NO by NH_3 over V_2O_5-WO_3/TiO_2 catalysts. Environ Technol Innov :. Article in press https://doi.org/10.1016/j.eti.2020.101209

Liu Y, Guo W (2021) SO_x factors as cell-state regulators in the mammary gland and breast cancer. Semin Cell Dev Biol 114:126–133. https://doi.org/10.1016/j.semcdb.2021.01.002

Liu SM, Guo RT, Sun P et al (2017) The enhancement of Zn resistance of Mn/TiO_2 catalyst for NH_3-SCR reaction by the modification with $Al_2(SO_4)_3$. J Taiwan Inst Chem Eng 78:370–377. https://doi.org/10.1016/j.jtice.2017.06.039

Liu Y, Zhao J, Lee JM (2018) Conventional and new materials for Selective Catalytic Reduction (SCR) of NO_x. ChemCatChem 10:1499–1511. https://doi.org/10.1002/cctc.201701414

Liu J, Sun M, Lin Q et al (2019a) Promotional effects of ethylenediamine on the low-temperature catalytic activity of selective catalytic oxidation of ammonia over Pt/$SiAlO_x$: states and particle sizes of Pt. Appl Surf Sci 481:1344–1351. https://doi.org/10.1016/j.apsusc.2019.03.199

Liu L, Su S, Xu K et al (2019b) Insights into the highly efficient Co modified MnSm/Ti catalyst for selective catalytic reduction of NO_x with NH_3 at low temperature. Fuel 255:115798. https://doi.org/10.1016/j.fuel.2019.115798

Liu K, Yu Q, Wang B et al (2020a) Binary copper-manganese based catalysts with urea for low-temperature selective catalytic reduction of NO: performance, characterization and mechanism. Appl Surf Sci 508:144755. https://doi.org/10.1016/J.APSUSC.2019.144755

Liu R, Zhou B, Liu L et al (2021) Enhanced catalytic oxidation of VOCs over porous Mn-based mullite synthesized by in-situ dismutation. J Colloid Interface Sci 585:302–311. https://doi.org/10.1016/j.jcis.2020.11.096

Liu L, Xu K, Su S, et al (2020b) Efficient Sm modified Mn/TiO_2 catalysts for selective catalytic reduction of NO with NH_3 at low temperature. Appl Catal A Gen 592:. https://doi.org/10.1016/j.apcata.2020.117413

Ma H, Schneider WF (2020) DFT and microkinetic comparison of Pt, Pd and Rh-catalyzed ammonia oxidation. J Catal 383:322–330. https://doi.org/10.1016/j.jcat.2020.01.029

Ma X, Hou Y, Yang L, Lv H (2021a) Adsorption behaviors of VOCs under coal-combustion flue gas environment using activated carbon injection coupled with bag filtering system. Colloids Surfaces A Physicochem Eng Asp 627:127158. https://doi.org/10.1016/j.colsurfa.2021.127158

Ma X, Zhang T, Ji C et al (2021b) Threats to human health and ecosystem: looking for air-pollution related damage since 1990. Renew Sustain Energy Rev 145:111146. https://doi.org/10.1016/j.rser.2021.111146

Manisalidis I, Stavropoulou E, Stavropoulos A, Bezirtzoglou E (2020) Environmental and health impacts of air pollution: a review. Front Public Health 0:14. https://doi.org/10.3389/FPUBH.2020.00014

Martinez-Oviedo A, Kshetri YK, Joshi B, Lee SW (2021) Surface modification of blue TiO_2 with silane coupling agent for NO_x abatement. Prog Nat Sci Mater Int 31:230–238. https://doi.org/10.1016/j.pnsc.2021.02.001

Méausoone C, El Khawaja R, Tremolet G et al (2019) In vitro toxicological evaluation of emissions from catalytic oxidation removal of industrial VOCs by air/liquid interface (ALI) exposure system in repeated mode. Toxicol Vitr 58:110–117. https://doi.org/10.1016/j.tiv.2019.03.030

Mergbi M, Galloni MG, Aboagye D et al (2023) Valorization of lignocellulosic biomass into sustainable materials for adsorption and photocatalytic applications in water and air remediation. Springer, Berlin Heidelberg

Montero-Montoya R, López-Vargas R, Arellano-Aguilar O (2018) Volatile organic compounds in air: sources, distribution, exposure and associated illnesses in children. Ann Glob Heal 84:225–238. https://doi.org/10.29024/aogh.910

Munsif R, Zubair M, Aziz A, Zafar MN (2021) Industrial air emission pollution: potential sources and sustainable mitigation. Environ Emiss. https://doi.org/10.5772/INTECHOPEN.93104

Nakamura K, Muramatsu T, Ogawa T, Nakagaki T (2021) Prediction of de-NO_x performance using monolithic SCR catalyst under load following operation of natural gas-fired combined cycle power plants. Energy 227:120383. https://doi.org/10.1016/j.energy.2021.120383

Nassos S, Elm Svensson E, Boutonnet M, Järås SG (2007) The influence of Ni load and support material on catalysts for the selective catalytic oxidation of ammonia in gasified biomass. Appl Catal B Environ 74:92–102. https://doi.org/10.1016/j.apcatb.2007.01.015

Naveenkumar R, Ramesh Kumar S, Pushyanthkumar G, Senthil Kumaran S (2020) NO_x, CO & HC control by adopting activated charcoal enriched filter in catalytic converter of diesel engine. Mater Today Proc 22:2283–2290. https://doi.org/10.1016/j.matpr.2020.03.349

Neha PR, Vir Singh S (2020) Catalytic abatement of CO, HCs and soot emissions over spinel-based catalysts from diesel engines: an overview. J Environ Chem Eng 8:103627. https://doi.org/10.1016/j.jece.2019.103627

Ojstršek A, Fakin D, Hribernik S, et al (2020) Electrospun nanofibrous composites from cellulose acetate / ultra-high silica zeolites and their potential for VOC adsorption from air. Carbohydr Polym 236:. https://doi.org/10.1016/j.carbpol.2020.116071

Ongari D, Tiana D, Stoneburner SJ et al (2017) Origin of the strong interaction between polar molecules and copper(II)

paddle-wheels in metal organic frameworks. J Phys Chem C 121:15135–15144. https://doi.org/10.1021/ACS.JPCC.7B02302

Oton LF, Oliveira AC, de Araujo JCS et al (2020) Selective catalytic reduction of NO$_x$ by CO (CO-SCR) over metal-supported nanoparticles dispersed on porous alumina. Adv Powder Technol 31:464–476. https://doi.org/10.1016/J.APT.2019.11.003

Ou R, Zhu W, Li L, et al (2021) Boosted capture of volatile organic compounds in adsorption capacity and selectivity by rationally exploiting defect-engineering of UiO-66(Zr). Sep Purif Technol 266:. https://doi.org/10.1016/j.seppur.2020.118087

Pappas DK, Boningari T, Boolchand P, Smirniotis PG (2016) Novel manganese oxide confined interweaved titania nanotubes for the lowerature selective catalytic reduction (SCR) of NOx by NH$_3$. J Catal 334:1–13. https://doi.org/10.1016/j.jcat.2015.11.013

Patel VK, Sharma S (2021) Effect of oxide supports on palladium based catalysts for NO reduction by H$_2$-SCR. Catal Today 375:591–600. https://doi.org/10.1016/j.cattod.2020.04.006

Peng S, Yang X, Strong J et al (2020) MnO$_2$-decorated N-doped carbon nanotube with boosted activity for low-temperature oxidation of formaldehyde. J Hazard Mater 396:122750. https://doi.org/10.1016/j.jhazmat.2020.122750

Pinzón M, Ruiz-López E, Romero A et al (2021) Electrochemical activation of Ru catalyst with alkaline ion conductors for the catalytic decomposition of ammonia. Mol Catal 511:111721. https://doi.org/10.1016/j.mcat.2021.111721

Piumetti M, Fino D, Russo N (2015) Mesoporous manganese oxides prepared by solution combustion synthesis as catalysts for the total oxidation of VOCs. Appl Catal B Environ 163:277–287. https://doi.org/10.1016/J.APCATB.2014.08.012

Plata-Gryl M, Momotko M, Makowiec S, Boczkaj G (2022) Characterization of diatomaceous earth coated with nitrated asphaltenes as superior adsorbent for removal of VOCs from gas phase in fixed bed column. Chem Eng J 427:130653. https://doi.org/10.1016/j.cej.2021.130653

Puri P, Nandar SK, Kathuria S, Ramesh V (2017) Effects of air pollution on the skin: a review. Indian J Dermatol Venereol Leprol 83:415–423. https://doi.org/10.4103/0378-6323.199579

Qi G, Gatt JE, Yang RT (2004) Selective catalytic oxidation (SCO) of ammonia to nitrogen over Fe-exchanged zeolites prepared by sublimation of FeCl$_3$. J Catal 226:120–128. https://doi.org/10.1016/j.jcat.2004.05.023

Qu Z, Fan R, Wang Z et al (2015) Selective catalytic oxidation of ammonia to nitrogen over MnO$_2$ prepared by urea-assisted hydrothermal method. Appl Surf Sci 351:573–579. https://doi.org/10.1016/j.apsusc.2015.05.154

Rahmaninejad F, Gavaskar VS, Abbasian J (2012) Dry regenerable CuO/γ-Al$_2$O$_3$ catalyst for simultaneous removal of SO$_x$ and NO$_x$ from flue gas. Appl Catal B Environ 119–120:297–303. https://doi.org/10.1016/j.apcatb.2012.03.005

Roberts W (2021) Air pollution and skin disorders. Int J Women's Dermatology 7:91–97. https://doi.org/10.1016/j.ijwd.2020.11.001

Roy S, Baiker A (2009) NO$_x$ Storage-reduction catalysis: from mechanism and materials properties to storage-reduction performance. Chem Rev 109:4054–4091. https://doi.org/10.1021/cr800496f

Roy S, Hegde MS (2008) Pd ion substituted CeO$_2$: a superior de-NO$_x$ catalyst to Pt or Rh metal ion doped ceria. Catal Commun 9:811–815. https://doi.org/10.1016/J.CATCOM.2007.09.019

Roy S, Aarthi T, Hegde MS, Madras G (2007a) Kinetics of photocatalytic reduction of NO by CO with Pd^{2+}-ion-substituted nano-TiO$_2$. Ind Eng Chem Res 46:5798–5802. https://doi.org/10.1021/ie0704593

Roy S, Hegde MS, Ravishankar N, Madras G (2007b) Creation of redox adsorption sites by Pd^{2+} ion substitution in nanoTiO$_2$ for high photocatalytic activity of CO oxidation, NO reduction, and NO decomposition. J Phys Chem C 111:8153–8160. https://doi.org/10.1021/jp066145v

Roy S, Marimuthu A, Hegde MS, Madras G (2007c) High rates of CO and hydrocarbon oxidation and NO reduction by CO over Ti$_{0.99}$Pd$_{0.01}$O$_{1.99}$. Appl Catal B Environ 73:300–310. https://doi.org/10.1016/J.APCATB.2007.01.003

Roy S, Marimuthu A, Hegde MS, Madras G (2007d) High rates of NO and N$_2$O reduction by CO, CO and hydrocarbon oxidation by O$_2$ over nano crystalline Ce$_{0.98}$Pd$_{0.02}$O$_{2−\delta}$: Catalytic and kinetic studies. Appl Catal B Environ 71:23–31. https://doi.org/10.1016/J.APCATB.2006.08.005

Roy S, Hegde MS, Sharma S et al (2008a) Low temperature NO$_x$ and N$_2$O reduction by H$_2$: mechanism and development of new nanocatalysts. Appl Catal B Environ 84:341–350. https://doi.org/10.1016/J.APCATB.2008.04.008

Roy S, Marimuthu A, Deshpande PA et al (2008b) Selective catalytic reduction of NO$_x$: mechanistic perspectives on the role of base metal and noble metal ion substitution. Ind Eng Chem Res 47:9240–9247. https://doi.org/10.1021/ie8010879

Roy S, Marimuthu A, Hegde MS, Madras G (2008c) NO reduction by H$_2$ over nano-Ce$_{0.98}$Pd$_{0.02}$O$_{2−\delta}$. Catal Commun 9:101–105. https://doi.org/10.1016/J.CATCOM.2007.05.031

Roy S, Viswanath B, Hegde MS, Madras G (2008d) Low-temperature selective catalytic reduction of NO with NH$_3$ over Ti$_{0.9}$M$_{0.1}$O$_{2-\delta}$ (M) Cr, Mn, Fe Co, Cu). J Phys Chem C 112:6002–6012

Roy S, Hegde MS, Madras G (2009) Catalysis for NO$_x$ abatement. Appl Energy 86:2283–2297. https://doi.org/10.1016/J.APENERGY.2009.03.022

Roy S, van Vegten N, Baiker A (2010) Single-step flame-made Pt/MgAl$_2$O$_4$ – A NO$_x$ storage-reduction catalyst with unprecedented dynamic behavior and high thermal stability. J Catal 271:125–131. https://doi.org/10.1016/J.JCAT.2010.02.017

Roy S, van Vegten N, Maeda N, Baiker A (2012) NO$_x$ storage and reduction over flame-made M/MgAl$_2$O$_4$ (M = Pt, Pd, and Rh): a comparative study. Appl Catal B Environ 119–120:279–286. https://doi.org/10.1016/J.APCATB.2012.03.008

Rutkowska M, Pacia I, Basąg S et al (2017) Catalytic performance of commercial Cu-ZSM-5 zeolite modified by desilication in NH$_3$-SCR and NH$_3$-SCO processes. Microporous Mesoporous Mater 246:193–206. https://doi.org/10.1016/j.micromeso.2017.03.017

Rutkowska M, Duda M, Macina D et al (2019) Mesoporous Beta zeolite functionalisation with FexCry oligocations; catalytic activity in the NH$_3$–SCO process. Microporous Mesoporous Mater 278:1–13. https://doi.org/10.1016/j.micromeso.2018.11.003

Sabzehmeidani MM, Mahnaee S, Ghaedi M et al (2021) Carbon based materials: a review of adsorbents for inorganic and organic compounds. Mater Adv 2:598–627. https://doi.org/10.1039/d0ma00087f

Saqlain S, Cha BJ, Kim SY et al (2021) Impact of humidity on the removal of volatile organic compounds over Fe loaded TiO$_2$ under visible light irradiation: insight into photocatalysis mechanism by operando DRIFTS. Mater Today Commun 26:102119. https://doi.org/10.1016/j.mtcomm.2021.102119

Sato K, Tomonaga H, Yamamoto T et al (2016) A synthetic pseudo-Rh: NO$_x$ reduction activity and electronic structure of Pd-Ru solid-solution alloy nanoparticles. Sci Rep 6:28265. https://doi.org/10.1038/srep28265

Sekiguchi K, Morinaga W, Sakamoto K et al (2010) Degradation of VOC gases in liquid phase by photocatalysis at the bubble interface. Appl Catal B Environ 97:190–197. https://doi.org/10.1016/j.apcatb.2010.03.039

Shang K, Ren J, Zhang Q et al (2021) Successive treatment of benzene and derived byproducts by a novel plasma catalysis-adsorption

process. J Environ Chem Eng 9:105767. https://doi.org/10.1038/srep28265

Shao Q, Dong H, Zhang J et al (2021) Manganese supported on controlled dealumination Y-zeolite for ozone catalytic oxidation of low concentration toluene at low temperature. Chemosphere 271:129604. https://doi.org/10.1016/j.chemosphere.2021.129604

Shi W, Bi J, Liu R et al (2021a) Decrease in the chronic health effects from PM2.5 during the 13th Five-Year Plan in China: impacts of air pollution control policies. J Clean Prod 317:128433. https://doi.org/10.1016/j.jclepro.2021.128433

Shi Y, Chu Q, Xiong W et al (2021b) A new type bimetallic NiMn-MOF-74 as an efficient low-temperatures catalyst for selective catalytic reduction of NO by CO. Chem Eng Process - Process Intensif 159:108232. https://doi.org/10.1016/j.cep.2020.108232

Shi Y, Wang J, Zhou R (2021c) Pt-support interaction and nanoparticle size effect in Pt/CeO$_2$–TiO$_2$ catalysts for low temperature VOCs removal. Chemosphere 265:129127. https://doi.org/10.1016/j.chemosphere.2020.129127

Shi Y, Zhang L, Li W et al (2021) Association between long-term exposure to ambient air pollution and clinical outcomes among patients with heart failure: findings from the China PEACE Prospective Heart Failure Study. Ecotoxicol Environ Saf 222:112517. https://doi.org/10.1016/j.ecoenv.2021.112517

Si H, Zhou M, Fang Y et al (2021) Photocatalytic concrete for NO$_x$ degradation: influence factors and durability. Constr Build Mater 298:123835. https://doi.org/10.1016/j.conbuildmat.2021.123835

Skowron A, Lee DS, De LRR et al (2021) (2021) Greater fuel efficiency is potentially preferable to reducing NO$_x$ emissions for aviation's climate impacts. Nat Commun 121(12):1–8. https://doi.org/10.1038/s41467-020-20771-3

Song S, Jiang S (2012) Selective catalytic oxidation of ammonia to nitrogen over CuO/CNTs: the promoting effect of the defects of CNTs on the catalytic activity and selectivity. Appl Catal B Environ 117–118:346–350. https://doi.org/10.1016/j.apcatb.2012.01.030

Streets DG, Zhang Q, Wang L et al (2006) Revisiting China's CO emissions after the Transport and Chemical Evolution over the Pacific (TRACE-P) mission: synthesis of inventories, atmospheric modeling, and observations. J Geophys Res Atmos 111:D14. https://doi.org/10.1029/2006JD007118

Sun M, Wang S, Li Y et al (2017a) Promotion of catalytic performance by adding W into Pt/ZrO$_2$ catalyst for selective catalytic oxidation of ammonia. Appl Surf Sci 402:323–329. https://doi.org/10.1016/j.apsusc.2016.12.241

Sun M, Wang S, Li Y et al (2017b) Promotion of catalytic performance by adding Cu into Pt/ZSM-5 catalyst for selective catalytic oxidation of ammonia. J Taiwan Inst Chem Eng 78:401–408. https://doi.org/10.1016/j.jtice.2017.06.045

Tan W, Chen F, Gong L et al (2016) The role of ceria in LSM-GDC composite cathode for electrochemical reduction of nitric oxide. Appl Catal B Environ 197:244–253. https://doi.org/10.1016/j.apcatb.2016.02.029

Tan W, Wang J, Cai Y et al (2022) Molybdenum oxide as an efficient promoter to enhance the NH$_3$-SCR performance of CeO$_2$-SiO$_2$ catalyst for NO$_x$ removal. Catal Today 397–399:475–483. https://doi.org/10.1016/j.cattod.2021.07.007

Tang X, Wang C, Gao F et al (2020) Effect of hierarchical element doping on the low-temperature activity of manganese-based catalysts for NH$_3$-SCR. J Environ Chem Eng 8:104399. https://doi.org/10.1016/j.jece.2020.104399

Tian B, Ma S, Zhan Y et al (2021a) Stability and catalytic activity to NO$_x$ and NH$_3$ of single-atom manganese catalyst with graphene-based substrate: a DFT study. Appl Surf Sci 541:148460. https://doi.org/10.1016/j.apsusc.2020.148460

Tian S, Zhan S, Lou Z et al (2021b) Electrodeposition synthesis of 3D-NiO$_{1-\delta}$ flowers grown on Ni foam monolithic catalysts for

efficient catalytic ozonation of VOCs. J Catal 398:1–13. https://doi.org/10.1016/j.jcat.2021.04.011

Tsimpidi AP, Trail M, Hu Y et al (2012) Modeling an air pollution episode in northwestern United States: identifying the effect of nitrogen oxide and volatile organic compound emission changes on air pollutants formation using direct sensitivity analysis. J Air Waste Manag Assoc 62:1150–1165. https://doi.org/10.1080/10962247.2012.697093

Ueno Y, Horiuchi T, Morimoto T, Niwa O (2001) Microfluidic device for airborne BTEX detection. Anal Chem 73:4688–4693. https://doi.org/10.1021/ac010210+

Wang C-C, Yang Y-J, Jiang J-C (2009) DFT study of NH$_x$ (x = 1–3) adsorption on RuO2(110) surfaces. J Phys Chem C 113:2816–2821. https://doi.org/10.1021/JP8062355

Wang Z, Qu Z, Quan X et al (2013) Selective catalytic oxidation of ammonia to nitrogen over CuO-CeO$_2$ mixed oxides prepared by surfactant-templated method. Appl Catal B Environ 134–135:153–166. https://doi.org/10.1016/j.apcatb.2013.01.029

Wang T, Zhu C, Liu H et al (2018a) Performance of selective catalytic reduction of NO with NH$_3$ over natural manganese ore catalysts at low temperature. Environ Technol 39:317–326. https://doi.org/10.1080/09593330.2017.1300190

Wang Y, Yang D, Li S et al (2018b) Ru/hierarchical HZSM-5 zeolite as efficient bi-functional adsorbent/catalyst for bulky aromatic VOCs elimination. Microporous Mesoporous Mater 258:17–25. https://doi.org/10.1016/j.micromeso.2017.08.052

Wang F, Shen B, Zhu S, Wang Z (2019a) Promotion of Fe and Co doped Mn-Ce/TiO$_2$ catalysts for low temperature NH$_3$-SCR with SO$_2$ tolerance. Fuel 249:54–60. https://doi.org/10.1016/j.fuel.2019.02.113

Wang HM, Ning P, Zhang QL et al (2019b) Effect of different RuO$_2$ contents on selective catalytic oxidation of ammonia over RuO$_2$-Fe$_2$O$_3$ catalysts. Ranliao Huaxue Xuebao/journal Fuel Chem Technol 47:215–223. https://doi.org/10.1016/s1872-5813(19)30011-8

Wang Z, Sun Q, Wang D et al (2019c) Hollow ZSM-5 zeolite encapsulated Ag nanoparticles for SO$_2$-resistant selective catalytic oxidation of ammonia to nitrogen. Sep Purif Technol 209:1016–1026. https://doi.org/10.1016/j.seppur.2018.09.045

Wang ZY, Guo RT, Shi X et al (2020) The superior performance of CoMnO$_x$ catalyst with ball-flowerlike structure for low-temperature selective catalytic reduction of NO$_x$ by NH$_3$. Chem Eng J 381:122753. https://doi.org/10.1016/j.cej.2019.122753

Wang C, Ren D, Harle G et al (2021a) Ammonia removal in selective catalytic oxidation: influence of catalyst structure on the nitrogen selectivity. J Hazard Mater 416:125782. https://doi.org/10.1016/j.jhazmat.2021.125782

Wang F, Zhu Y, Li Z et al (2021b) Promoting effect of acid sites on NH$_3$-SCO activity with water vapor participation for Pt-Fe/ZSM-5 catalyst. Catal Today 376:311–317. https://doi.org/10.1016/j.cattod.2020.06.039

Wang H, Lin M, Murayama T et al (2021c) Selective catalytic oxidation of ammonia to nitrogen over zeolite-supported Pt-Au catalysts: effects of alloy formation and acid sites. J Catal 402:101–113. https://doi.org/10.1016/j.jcat.2021.08.002

Wang X, Tan W, Guo K et al (2021d) Evaluation of manganese oxide octahedral molecular sieves for CO and C$_3$H$_6$ oxidation at diesel exhaust conditions. Front Environ Chem 2:72250. https://doi.org/10.3389/fenvc.2021.672250

Wantz E, Kane A, Lhuissier M et al (2021) A mathematical model for VOCs removal in a treatment process coupling absorption and biodegradation. Chem Eng J 423:130106. https://doi.org/10.1016/j.cej.2021.130106

Wei Y, Fan H, Wang R (2018) Transition metals (Co, Zr, Ti) modified iron-samarium oxide as efficient catalysts for selective

catalytic reduction of NO$_x$ at low-temperature. Appl Surf Sci 459:63–73. https://doi.org/10.1016/j.apsusc.2018.07.151

Wu Z, Deng J, Xie S et al (2016) Mesoporous Cr$_2$O$_3$-supported Au–Pd nanoparticles: high-performance catalysts for the oxidation of toluene. Microporous Mesoporous Mater 224:311–322. https://doi.org/10.1016/J.MICROMESO.2015.11.061

Wu R, Li L, Zhang N et al (2021) Enhancement of low-temperature NH$_3$-SCR catalytic activity and H$_2$O & SO$_2$ resistance over commercial V$_2$O$_5$-MoO$_3$/TiO$_2$ catalyst by high shear-induced doping of expanded graphite. Catal Today 376:302–310. https://doi.org/10.1016/j.cattod.2020.04.051

Xu H, Yan N, Qu Z et al (2017) Gaseous heterogeneous catalytic reactions over Mn-based oxides for environmental applications: a critical review. Environ Sci Technol 51:8879–8892. https://doi.org/10.1021/ACS.EST.6B06079

Xu Y, Wu X, Lin Q et al (2019) SO$_2$ promoted V$_2$O$_5$-MoO$_3$/TiO$_2$ catalyst for NH$_3$-SCR of NO$_x$ at low temperatures. Appl Catal A Gen 570:42–50. https://doi.org/10.1016/j.apcata.2018.10.040

Xue Y, Sun W, Wang Q et al (2018) Sparsely loaded Pt/MIL-96(Al) MOFs catalyst with enhanced activity for H$_2$-SCR in a gas diffusion reactor under 80 °C. Chem Eng J 335:612–620. https://doi.org/10.1016/J.CEJ.2017.11.011

Yan Q, Chen S, Zhang C et al (2018) Synthesis of Cu$_{0.5}$Mg$_{1.5}$Mn$_{0.5}$Al$_{0.5}$O$_x$ mixed oxide from layered double hydroxide precursor as highly efficient catalyst for low-temperature selective catalytic reduction of NO$_x$ with NH$_3$. J Colloid Interface Sci 526:63–74. https://doi.org/10.1016/j.jcis.2018.04.099

Yan DJ, Guo T, Yu Y, Chen ZH (2021) Lead poisoning and regeneration of Mn-Ce/TiO$_2$ catalysts for NH$_3$-SCR of NO$_x$ at low temperature. Ranliao Huaxue Xuebao/journal Fuel Chem Technol 49:113–120. https://doi.org/10.1016/S1872-5813(21)60003-8

Yang L, You X, Sheng Z et al (2018) The promoting effect of noble metal (Rh, Ru, Pt, Pd) doping on the performances of MnO$_x$-CeO$_2$ / graphene catalysts for the selective catalytic reduction of NO with NH$_3$ at low temperatures. New J Chem 42:11673. https://doi.org/10.1039/c8nj01417e

Yang W, Wang X, Song S, Zhang H (2019) Syntheses and applications of noble-metal-free CeO$_2$-based mixed-oxide nanocatalysts. Chem 5:1743–1774. https://doi.org/10.1016/j.chempr.2019.04.009

Yang B, Zhou J, Wang W et al (2020) Extraction and separation of tungsten and vanadium from spent V$_2$O$_5$–WO$_3$/TiO$_2$ SCR catalysts and recovery of TiO$_2$ and sodium titanate nanorods as adsorbent for heavy metal ions. Colloids Surfaces A Physicochem Eng Asp 601:124963. https://doi.org/10.1016/j.colsurfa.2020.124963

Yang J, Qin J, Guo Z et al (2021a) Zn-based metal organic framework derivative with uniform metal sites and hierarchical pores for efficient adsorption of formaldehyde. Chinese Chem Lett 32:1819–1822. https://doi.org/10.1016/j.cclet.2020.11.023

Yang M, Shen G, Wang Q et al (2021b) Roles of oxygen vacancies of CeO$_2$ and Mn-doped CeO$_2$ with the same morphology in benzene catalytic oxidation. Mol 26:6363. https://doi.org/10.3390/molecules26216363

Ye B, Kim J, Lee MJ et al (2021) Mn-Ce oxide nanoparticles supported on nitrogen-doped reduced graphene oxide as low-temperature catalysts for selective catalytic reduction of nitrogen oxides. Microporous Mesoporous Mater 310:110588. https://doi.org/10.1016/j.micromeso.2020.110588

Yu Q, Richter M, Li L et al (2010) The promotional effect of Cr on catalytic activity of Pt/ZSM-35 for H$_2$-SCR in excess oxygen. Catal Commun 11:955–959. https://doi.org/10.1016/J.CATCOM.2010.03.021

Yu X, Liu S, Lin G et al (2020) KOH-activated hydrochar with engineered porosity as sustainable adsorbent for volatile organic compounds. Colloids Surfaces A Physicochem Eng Asp 588:124372. https://doi.org/10.1016/j.colsurfa.2019.124372

Zeng Y, Gu L, Feng Y et al (2020) Morphologically uniform Pd/Fe$_x$Mn$_{3-x}$O$_4$-HP interfaces as the high-performance model catalysts for catalytic combustion of volatile organic compound. Appl Surf Sci 528:147006. https://doi.org/10.1016/j.apsusc.2020.147006

Zhang L, He H (2009) Mechanism of selective catalytic oxidation of ammonia to nitrogen over Ag/Al$_2$O$_3$. J Catal 268:18–25. https://doi.org/10.1016/j.jcat.2009.08.011

Zhang L, Zhang C, He H (2009) The role of silver species on Ag/Al$_2$O$_3$ catalysts for the selective catalytic oxidation of ammonia to nitrogen. J Catal 261:101–109. https://doi.org/10.1016/j.jcat.2008.11.004

Zhang Q, Wang H, Ning P et al (2017a) In situ DRIFTS studies on CuO-Fe$_2$O$_3$ catalysts for low temperature selective catalytic oxidation of ammonia to nitrogen. Appl Surf Sci 419:733–743. https://doi.org/10.1016/j.apsusc.2017.05.056

Zhang X, Gao B, Creamer AE et al (2017b) Adsorption of VOCs onto engineered carbon materials: a review. J Hazard Mater 338:102–123. https://doi.org/10.1016/j.jhazmat.2017.05.013

Zhang L, Yang C, Lv K et al (2019a) SPR effect of bismuth enhanced visible photoreactivity of Bi$_2$WO$_6$ for NO abatement. Cuihua Xuebao/chinese J Catal 40:755–764. https://doi.org/10.1016/s1872-2067(19)63320-6

Zhang LL, Chen XM, Liu CG (2019b) Reduction of N$_2$O by CO via Mans-van Krevelen mechanism over phosphotungstic acid supported single-atom catalysts: a density functional theory study. Inorg Chem 58:5221–5229. https://doi.org/10.1021/acs.inorgchem.9b00290

Zhang Y, Liu J, Xing H, Li J (2020a) Performance and fungal diversity of bio-trickling filters packed with composite media of polydimethylsiloxane and foam ceramics for hydrophobic VOC removal. Chemosphere 256:127093. https://doi.org/10.1016/j.chemosphere.2020.127093

Zhang Y, Zhao L, Duan J, Bi S (2020b) Insights into deNO$_x$ processing over Ce-modified Cu-BTC catalysts for the CO-SCR reaction at low temperature by in situ DRIFTS. Sep Purif Technol 234:116081. https://doi.org/10.1016/j.seppur.2019.116081

Zhang Z, Jiang C, Li D et al (2020c) Micro-mesoporous activated carbon simultaneously possessing large surface area and ultrahigh pore volume for efficiently adsorbing various VOCs. Carbon N Y 170:567–579. https://doi.org/10.1016/j.carbon.2020.08.033

Zhang X, Lv S, Zhang X et al (2021a) Improvement of the activity and SO$_2$ tolerance of Sb-modified Mn/PG catalysts for NH$_3$-SCR at a low temperature. J Environ Sci (China) 101:1–15. https://doi.org/10.1016/j.jes.2020.07.027

Zhang Z, Li R, Wang M, et al (2021b) Two steps synthesis of CeTiO$_x$ oxides nanotube catalyst: enhanced activity, resistance of SO$_2$ and H$_2$O for low temperature NH$_3$-SCR of NO$_x$. Appl Catal B Environ 282:. https://doi.org/10.1016/j.apcatb.2020.119542

Zhang Z, Li Y, Yang P et al (2021c) Improved NH$_3$-SCR deNO$_x$ activity and tolerance to H$_2$O & SO$_2$ at low temperature over the Nb$_m$Cu$_{0.1-m}$Ce$_{0.9}$O$_x$ catalysts: role of acidity by niobium doping. Fuel 303:121239. https://doi.org/10.1016/j.fuel.2021.121239

Zhao Z, Dai H, Deng J et al (2012) Three-dimensionally ordered macroporous La$_{0.6}$Sr$_{0.4}$FeO$_{3-\delta}$: high-efficiency catalysts for the oxidative removal of toluene. Microporous Mesoporous Mater 163:131–139. https://doi.org/10.1016/J.MICROMESO.2012.07.006

Zhao D, Gao Z, Xian H et al (2018) Addition of Pd on La$_{0.7}$Sr$_{0.3}$CoO$_3$ perovskite to enhance catalytic removal of NO$_x$. I&EC Res 57:521–531. https://doi.org/10.1021/acs.iecr.7b04399

Zhao G, Li M, Wang L et al (2020a) Environmentally-friendly tourmaline modified CeMnFeO$_x$ catalysts for low-temperature selective catalytic reduction of NO$_x$ with NH$_3$. Catal Today 355:385–396. https://doi.org/10.1016/j.cattod.2019.08.018

Zhao J, Xi W, Tu C et al (2020b) Catalytic oxidation of chlorinated VOCs over Ru/Ti$_x$Sn$_{1-x}$ catalysts. Appl Catal B Environ 263:118237. https://doi.org/10.1016/j.apcatb.2019.118237

Zhao W, Adeel M, Zhang P et al (2022) A critical review on surface-modified nano-catalyst application for the photocatalytic degradation of volatile organic compounds. Environ Sci Nano 9:61–80. https://doi.org/10.1039/d1en00955a

Zhao Q, Zheng Y, Song C et al (2020) Novel monolithic catalysts derived from in-situ decoration of Co$_3$O$_4$ and hierarchical Co$_3$O$_4$@MnO$_x$ on Ni foam for VOC oxidation. Appl Catal B Environ 265:118552. https://doi.org/10.1016/j.apcatb.2019.118552

Zhou G, Lan H, Wang H et al (2014) Catalytic combustion of PVOCs on MnO$_x$ catalysts. J Mol Catal A Chem 393:279–288. https://doi.org/10.1016/J.MOLCATA.2014.06.028

Zhou X, Yu F, Sun R et al (2020) Two-dimensional MnFeCo layered double oxide as catalyst for enhanced selective catalytic reduction of NO$_x$ with NH$_3$ at low temperature (25–150 °C). Appl Catal A Gen 592:117432. https://doi.org/10.1016/j.apcata.2020.117432

Zhu M, Wachs IE (2015) Iron-based catalysts for the high-temperature water−gas shift (HT-WGS) reaction: a review. ACS Catal 6:722–732. https://doi.org/10.1021/acscatal.5b02594

Zhu Z, Xu B (2022) Purification technologies for NO$_x$ removal from flue gas: a review. Separations 9:1–27. https://doi.org/10.3390/separations9100307

Zhu L, Zhong Z, Xue J et al (2018) NH$_3$-SCR performance and the resistance to SO$_2$ for Nb doped vanadium based catalyst at low temperatures. J Environ Sci (China) 65:306–316. https://doi.org/10.1016/j.jes.2017.06.033

Zhu H, Song S, Wang R (2020) Removal of nox by adsorption/decomposition on H$_3$PW$_{12}$O$_{406}$·H$_2$O/CeO$_2$ supported on ceria. Aerosol Air Qual Res 20:2273–2279. https://doi.org/10.4209/aaqr.2020.03.0110

Zou L, Luo Y, Hooper M, Hu E (2006) Removal of VOCs by photocatalysis process using adsorption enhanced TiO$_2$-SiO$_2$ catalyst. Chem Eng Process Process Intensif 45:959–964. https://doi.org/10.1016/j.cep.2006.01.014